MEE 482

Mars Aeolian Wind Tunnel Test Stand

Group #20

Group Member:

Haley Cummings

Advisors:

Dr. William Warmbrodt

Geoffrey Ament

Gina Willink

NASA Ames Rotorcraft Aeromechanics Division

Dr. Jenn-Terng Gau

Northern Illinois University

9 May 2016

Contents

Table of Figures

Table of Equations

Acknowledgments

I would like to first thank Dr. Gau, Dr. Majumdar, Dr. Coller, and Beatrice Kooken for working with me to make this senior design project possible

I would also like to thank Dr. William Warmbrodt, Geoffrey Ament, Gina Willink, and NASA Ames Research Center for giving me this opportunity and for helping me practically apply the theory I learn in school

Abstract

The exploration of Mars has long been a theme in science fiction entertainment. However, with successful NASA Mars rover missions such as Curiosity and Opportunity, this fiction has become a reality. As NASA prepares additional rovers to explore the Red Planet, the agency is looking for ways to make exploration more efficient. One solution is to use a small, lightweight, co-axial rotor helicopter to scout geographical conditions on the Martian surface. This type of flight is unprecedented, as no vehicle has flown in the Martian atmosphere. With that said, extensive experimentation is needed to develop such a vehicle. Initial testing has been completed on what has been dubbed the Mars Scout Helicopter (MSH), and the next phase of testing will include wind tunnel testing of the rotor in forward flight in a reduced pressure environment, simulating the atmosphere of Mars.

Nomenclature

Ames Research Center	ARC
Computational Fluid Dynamics	CFD
Computer Aided Design	CAD
Finite Element Analysis	FEA
Jet Propulsion Laboratory	JPL
Kilopounds per Square Inch	KSI
Mars Scout Helicopter	MSH
National Aeronautics and Space Administration	NASA
Rotor Computational Fluid Dynamics	RotCFD
Revolutions Per Minute	RPM
Science, Technology, Engineering, and Mathematics	STEM

Chapter 1

Introduction

The National Aeronautics and Space Administration (NASA) is known worldwide for its advances in space exploration and contributions to technological advancement in the medical field, the automotive industry, and countless other STEM fields. On November 26, 2011, NASA launched the Mars Rover known as Curiosity into the atmosphere, where it travelled 140 million miles over the course of eight months to land on Mars. The success of the Curiosity rover has been renowned worldwide.

Figure 1: MSH

In 2020, there will be another window of time where Mars and the Earth are in optimum position in their orbit around the sun to make another launch possible. Because of this, there is an ongoing mission being planned and designed for the next rover, which will launch in 2020. After seeing what has worked best, and what needs more fine tuning in the performance of the Curiosity rover, NASA is adding some features to the rover that will be launched in 2020. One such addition to the instrumentation is the inclusion of the Mars Scout Helicopter (MSH).

The Mars Scout Helicopter will act as "eyes in the sky" for the 2020 rover. It will be able to take off and land with the rover as its base. It will make short, two to three minute flights each day, and will take two dimensional pictures of the surrounding geography on Mars. It will then use those images to create a three dimensional portrayal of the landscape, which will then be sent back to the NASA engineers and scientists on earth, who will then choose the optimum geographical route for the rover to take. This will increase the distance that the rover can travel each day, and thus increase the number and quality of the scientific discoveries and experiments the 2020 rover can complete.

While much is known about flight, and specifically helicopter flight, here on earth, very little is known about how a helicopter would behave on the surface of Mars. It is known, however, that the atmosphere is much less dense compared to earth. This means that the helicopter rotor must spin nearly five times faster than typical helicopters spin on earth in order to displace the same amount of particles in the air to create lift. Because of this, much testing and simulating must be done regarding the design of the rotors and airfoils. This senior design project will focus on the design of the hardware that will be used to test the MSH rotor in various NASA facilities.

Figure 2: Hover Stand at JPL

In December of 2015, the Ames Research Center Aeromechanics Branch traveled to Pasadena, California in order to conduct rotor testing in JPL's Space Simulator. The rotor that was used is a 40-inch diameter blade. This blade was chosen because it is roughly the same size and generates roughly the same amount of lift as the actual MSH blade does. In the Space Simulator, the blade was mounted to a 12 foot tall vertical test stand, inside which a motor was suspended in order to spin the rotor. All of the data that was gathered from the tests conducted at JPL was strictly for a rotor in hover. Gathering data on rotor performance in hover was one of the first steps towards proof of concept and design evaluation. Many other flight conditions, however, must be tested and evaluated. The focus of this project was the design of a test stand that is able to test some of these other flight conditions. More specifically, the test stand of this project will be used to gather data for the rotor in forward flight in a reduced pressure Martian-like environment. These tests will be the first of their kind, as no testing for forward flight has been done in forward flight before. The wind tunnel that will be used is located in a chamber that is able to pump down to Martian pressure and beyond.

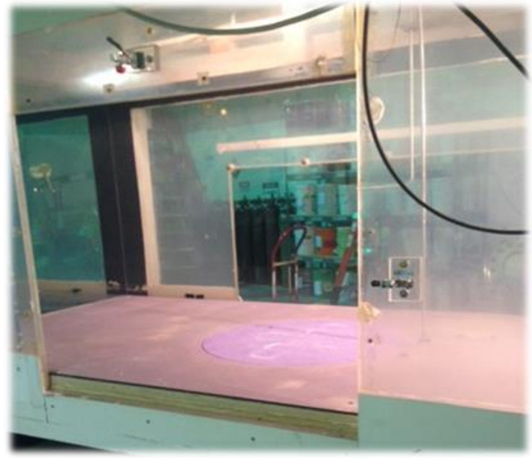

Figure 3: Aeolian Wind Tunnel

Chapter 2

Project Planning

This project was completed in conjunction with and under the supervision of NASA Ames Research Center, therefore the planning of this project was all theoretical until my arrival in California in January 2016. Prior to the official commencement of the internship, there was no set project to work on. The issues and specifications for each testing facility were still being discovered, with new problems being discovered and adjustments being made every day. Even so, however, a basic arbitrary project plan was laid out. In order to formulate a good project plan, several steps had to first be taken. Those included:

1) Identify the tasks
2) State the objectives
3) Estimate necessary resources
4) Develop steps to accomplish the tasks
5) Estimate costs

The relatively general overall objective of the project was to develop a piece of hardware that allows for the MSH rotor to be tested safely at the NASA Ames Research Center testing facility. It is of utmost importance that the piece of hardware be designed with safety in mind, because if a piece of the hardware or rotor were to break off and impact the

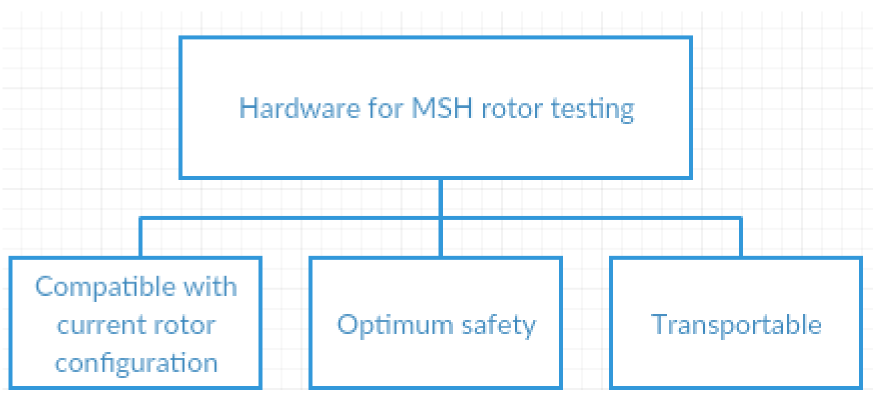

Figure 4: Function Flow Chart

wall of the test facility, it could prove fatal for the facility. Since the facility costs a substantial amount of money to maintain and repair, harm to the facility is obviously not desirable. In addition, the hardware will also need to be able to assist researchers in collecting data and information – both visually and through the use of instruments. If the hardware obstructs the gathering of data, it will ultimately defeat the purpose of the test. Finally, the hardware should be able to be transported and assembled with ease. Because the hardware is being used at Ames Research Center, and may be used in future testing at other facilities, it was beneficial to design the hardware so that it could be easily assembled. While transportability and ease of assembly was not a main concern, it was beneficial to consider it in the design process in order to benefit the overall MSH project.

The calculation of the estimated time that this project was predicted to take is slightly misleading, as my supervisor at Ames Research Center has had many, many interns and knows how to assign a project that will take approximately a semester to complete. However, as can be seen in Figure 4, the function flow chart was generally predicted for the project. From this, it was possible to use Equation 1, where A depends on compnay size, PC is product complexity, and D is degree of difficulty from one to three, three being most difficult, to predict how much time will be necessary for a given project. For this project, A will equal 20, PC is determined by Equation 2, and D will equal 2, as hardware for similar testing is available and can be used for reference. In Equation 2, j is equal to the level of the function diagram, and F_j is equal to the number of functions at level j. By solving Equation 1, the time required for this project is found to be 252.35 hours. If I were to spend my entire eight hour work day on this project, it would take me six weeks to complete the design of this project, according to this formula.

$$Time\ (in\ hours) = A * PC * D^{.85}$$

Equation 1

$$PC = \sum(j * F_j) = 1 * 1 + 2 * 3 = 7$$

Equation 2

The sequence of the tasks that are to be completed for this project can be found from the Gantt chart shown below. This gives an approximate timeline that will be followed for the project. However, after completing the project, it is interesting to return and review the above equation. This equation fails to take into account the many real world situations that designers and researchers encounter on a day to day basis. Because it often takes a few design iterations to clearly define the exact design specifications, the design is often modified or completely changed several times in the design process. The above equation also fails to take into account the many departments and different people that must give approval and feedback before more progress can be made. In addition, because all of the hardware pieces for this project had to be machined, much of the project was reliant on the machine shop's availability. When they were extremely busy, there was nothing that could necessarily be done to ensure that our hardware was top priority. Finally, safety meetings, all-hands meetings, and other such obligations are unavoidable in a company like NASA. While

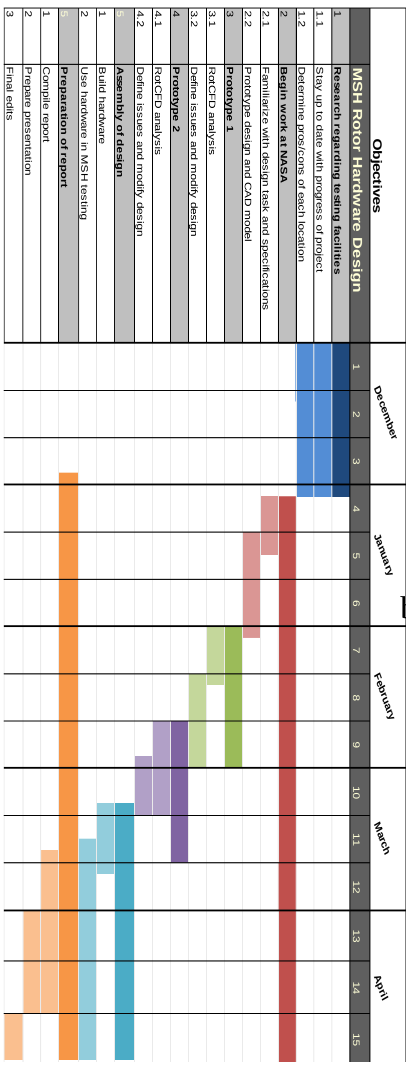

Figure 5: Gantt Chart

the above equation may be a decent tool for predicting the time frame of a project, it is in no way sufficient by itself to use for project planning exercises.

Previous Design Work

Prior to beginning work on the design of the Mars Aeolian Wind Tunnel Test Stand, I was involved in design work dealing with the design of hardware to assemble the 40 inch rotor hub. In the winter of 2015, the Mars Hover Test Stand was transported to JPL in order to conduct testing in JPL's Space Simulator. Prior to testing, the rotor hub had to be assembled and torqued to the proper specifications. The complete Standard Operating Procedure (SOP) for building up the hub can be found in the appendix. As can be seen, this process is slightly complicated, especially once one of the blades is mounted on the hub adapter. The entire assembly becomes quite unwieldy and difficult to manipulate. When the test team was at JPL, one of the blades allegedly sustained a micro-crack during the assembly process because in order to torque the bolts, it was necessary to hold on to the blades. The blades are not designed to sustain this kind of stress. Therefore, it became clear that it would be necessary to design a mechanical component to make the hub assembly easier and safer.

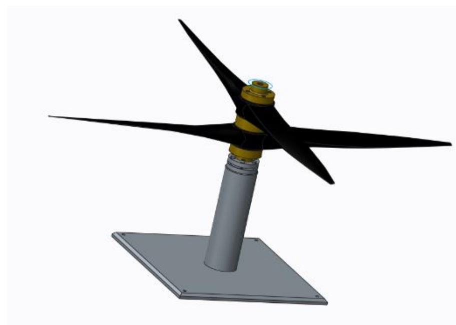

Figure 6: Mars Hub Stand


Figure 9: Shaft Collar (McMaster-Carr)

After much deliberation and discussion, it was determined that the optimum course of action would be to use a shrink-disc to hold the hub onto the hub stand that was being designed. A shrink-disc had previously been used in testing to secure the hub shaft to the motor shaft. This approach was chosen because the shrink-disc can be fastened to the hub stand using screws, which will ensure that the hub will not rotate while it is being assembled. Other ideas that were discussed included using a shaft collar and set screw (Figure 9), or a C-clamp type device. Ultimately, it was decided that the shrink-disc serves the same purpose as these devices, but it performs the task in the least complex manner.


Figure 8: Ringfeder Shrink-Disc


Figure 7: Cylindrical Piece

The Hub Stand was comprised of three components. The aforementioned shrink-disc was ordered from Ringfeder. The original hub was designed to be used with this particular shrink-disc, which meant that the sizing was already correct. The second component was the cylindrical piece, and the final component was the base plate onto which the cylindrical piece is attached. Each piece was designed specifically to be used with the hub and Ringfeder shrink-disc. The material chosen for the cylinder was 6061 Aluminum, and the material for the base plate was chosen to be A36 Steel. The cylindrical piece is 10.75 inches tall. This height was deemed a proper height because allows the hub to be at about the height of an average person’s arm during hub assembly if the Hub Stand is sitting on a table. The cylinder is attached to the base by four bolts, and has a small cylinder extruded out of the top

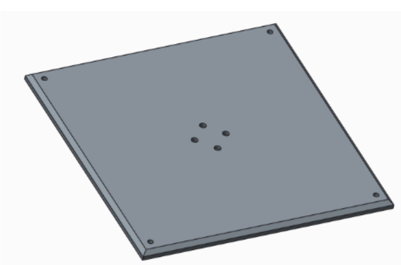
Figure 10: Base Plate

end. This small cylinder is what the hub is fixed to by the shrink-disc. There is a fillet between the small cylinder and the large cylinder to reduce the stress concentration.

The base plate was designed to be versatile. It can be fixed to a table using a C-Clamp, or it was also designed so that it can be mounted to 80/20. This ability to use the Hub Stand in conjunction with 80/20 makes it flexible. It can be used in any environment, with or without a table.

In-depth analysis was performed on each piece of the hardware to ensure an adequate safety factor. Analysis was performed mainly using hand calculations in a Microsoft Excel spreadsheet, but additional analysis was performed using PTC Creo's Finite Element Analysis package. The required safety factor imposed by Senior Mechanical Engineer Gina Willink was 4. However, in most cases, the safety factor was well beyond this number, and in many cases was above 500. Such high factors of safety are not necessary, but they inspire confidence in the design. There was some concern regarding the fillet between the small cylinder and the large cylinder, but sufficient analysis was completed to ensure that this fillet would not pose any problems. The analysis shown to the right is with a force of 80 lbs acting horizontally on the small cylinder. The highest stress is less than 700 psi and gives a safety factor of 85. A simulation was run to find the highest amount of force that could be placed on the cylinder without breaching the ultimate tensile strength, and it was found that nearly 70000 lbs of force could be placed on the small cylinder. The hub stand will never sustain such a high force, as the stand is merely being used to assemble the hub. Additional analysis, including tipping condition and shear on the bolts, can be found in the appendix.

Figure 11: FEA Analysis on Cylinder

The design of the Mars Hub Stand was only a small part of the overarching project. The stand, however, will prove instrumental as testing continues. It allows for much easier assembly and disassembly of the hub, and ensures that no additional damage is incurred on the blades due to assembly. Complete drawings of the stand can be found in the appendix.

Chapter 3

Design Specifications

In order to clearly define a design procedure and plan, it is necessary to define the design specifications of the project. These are often given by the customer and refined by the engineer. In

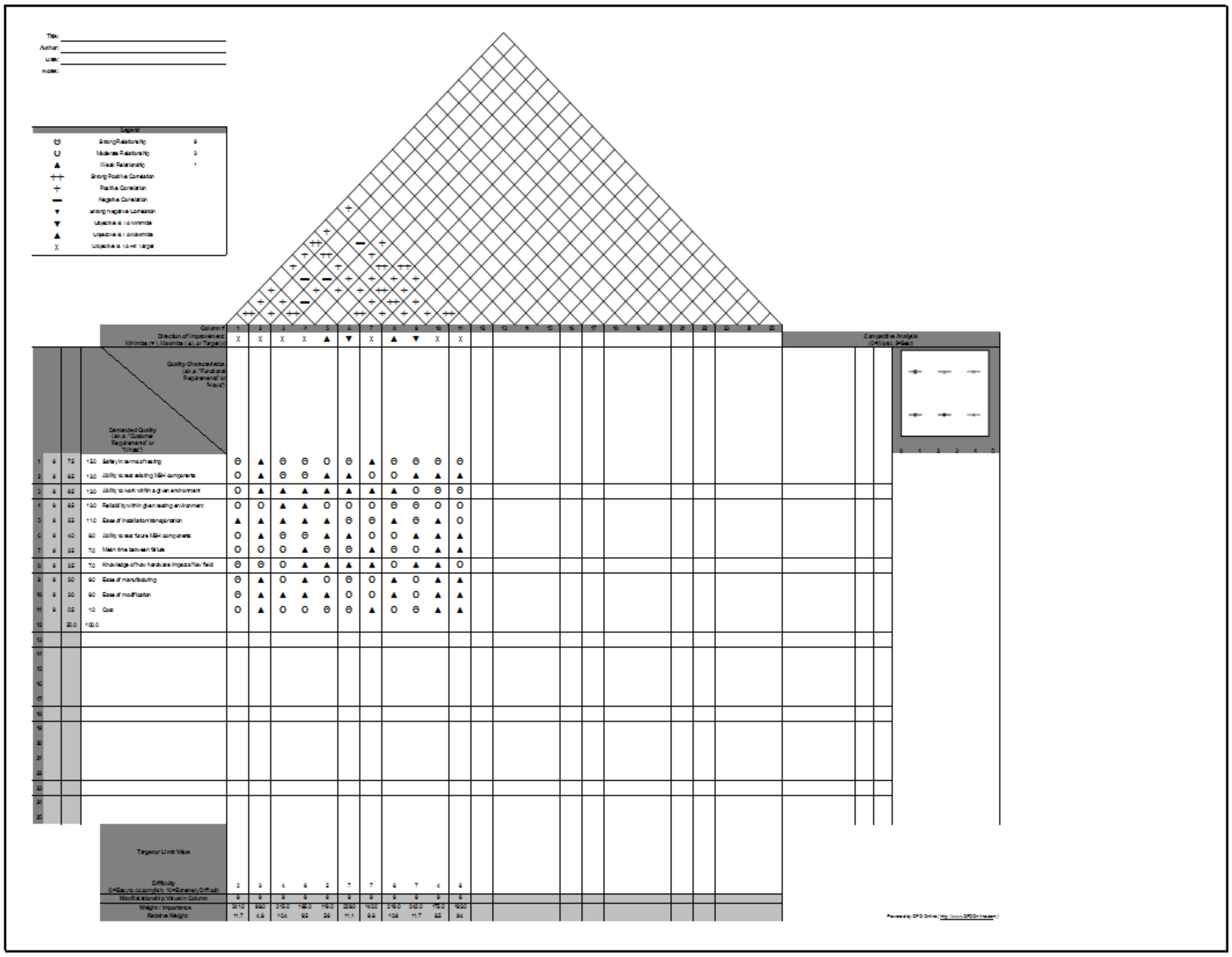

Figure 12: House of Quality

this case, many of the design specifications are defined because of the conditions of the Martian atmosphere. Additional specifications are given because of the functions of the MSH. Because the multiple specifications have various amounts of importance, the best way to organize and view the given specifications is in what is called a house of quality. This chart can be seen in Figure 12.

From the house of quality, it can be seen that two of the most important aspects of the design are the CAD model and no loose or unnecessary parts in the design. The CAD model is useful because it will allow the design to fit with the current MSH rotor design, as well as any future rotor designs. No loose or unnecessary parts will ensure the design is simple, yet effective, and that the rotor will be in a safe testing environment. As previously noted, this is imperative because the test facilities are very fragile and cannot sustain damage due to loose parts flying off of the apparatus. The design specifications of the MSH (Young, Aiken, Derby, Demblewski, & Navarrete) are as follows:

- Disc Loading: 4 N/m^2
- Vehicle Mass: 2 kg
- Rotor Radius: ~.55 m
- Adequate performance at low Reynold's number
- Adequate performance at high Mach number
- Adequate mechanical properties to last at least two earth years (up to fifteen earth years) with one flight lasting ~3 minutes per day (ex. Curiosity rover designed to last two years, potential to last up to 15 years based on power system)
- Adequate mechanical properties to consistently perform at 2400-3000 RPM

Additional design tasks (Chen, 2015) that will be necessary include:

- Perform CFD analysis using RotCFD on hardware design with and without rotor
- Analyze whether a single rotor can be used to simulate a co-axial configuration
- Perform testing in simulated Martian atmosphere
- Additional research regarding Martian atmosphere and the constraints that said atmosphere provides (ex. Characteristics of flow fields at Martian atmospheric pressures etc.)

The design specifications and design tasks were all implemented in the house of quality to determine the relationships and importance of each.

Once Larry Young of the ARC Aeromechanics Branch began to consider the next step in MSH testing, it became apparent to him that the next step in testing would be to test MSH rotor performance in forward flight in a reduced atmospheric environment like that of Mars. Forward flight occurs when the blades are pitched in such a way that the lift generated propels the helicopter forward instead of solely up and down, like in hover. Mr. Young wants to quantify the interference effects felt by the rotor, as well as gather data on rotor thrust, torque, and power. In addition, Mr. Young wants to prove the capability of the Ames facilities to test forward flight. JPL is at the forefront of readying the MSH for the 2020 launch. JPL has excellent facilities, but by showing JPL that Ames is ready and able to test forward flight in Mars conditions, JPL must consider the advantages to testing in a facility that already has had preliminary checkouts. This could potentially help JPL with their flight checkouts and speed up their design process to keep them on schedule. As Mr. Young began considering where to conduct these forward flight tests, he began talking to the Mars Aeolian Wind Tunnel operators and scientists about using their chamber and wind tunnel. The wind tunnel is mainly used for testing how Martian dirt and dust reacts to the Martian winds in a reduced pressure environment. It was quickly determined that this tunnel would provide the proper environment and conditions for the desired testing.

While the Mars Aeolian Wind Tunnel is an excellent candidate for the desired testing, it does present some design challenges, and thus some design specifications. In addition, several design specifications were proposed by Mr. Young as well. The tunnel is only 38 inches tall and 48 inches wide, which limits the orientations that the blades can be mounted in the tunnel, as the blades are 40 inches in diameter. Because of this, two test orientations were required. The first required that the blades be mounted so that they are at a 0° angle relative to the tunnel floor. The second configuration requires that the blades be mounted at a 45° angle relative to the tunnel floor.

MECHANICAL PROPERTIES

Typical Mechanical Properties*

Property	A	H 900	Condition H 925	H 1025	H 1075	H 1150	H 1150-M
UTS, ksi (MPa)							
Longitudinal	161 (1110)	209 (1438)	181 (1249)	174 (1200)	162 (1114)	150 (1035)	136 (938)
Transverse	162 (1116)	213 (1466)	184 (1272)	175 (1204)	162 (1114)	152 (1050)	137 (944)
0.2% YS, ksi (MPa)							
Longitudinal	140 (963)	201 (1385)	175 (1208)	171 (1176)	160 (1102)	140 (967)	111 (765)
Transverse	143 (988)	202 (1393)	177 (1222)	171 (1176)	161 (1112)	146 (1009)	111 (765)
Elongation, % in 2" (50.8 mm)							
Longitudinal	8.4	10.1	12.2	12.2	12.8	14.6	18.8
Transverse	7.6	9.4	9.8	9.3	11.4	13.1	17.8
Hardness, Rockwell C							
Longitudinal	35	46	41	40	38	36	31
Transverse	35	46	42	39	38	36	31

Figure 13: 15-5 Stainless Steel Mechanical Properties (AKSteel, 2007)

In order to test in forward flight, the blades have to be pitched into and out of the wind by 10° in each direction. Another design specification that was given because of the necessary blade pitch to test in forward flight was that there be an actuator attached to the motor assembly that forces the blades forward and backward relative to wind direction by 10°. The actuator would have to be remote controlled so that the blade pitch could be controlled from outside the reduced atmosphere chamber.

Mr. Young hoped to run his testing at 3000 RPM, which, in the given Mars conditions with the given rotor specifications, generates 150 pounds of lift. If a blade were to break, the resultant force felt by the test stand and its components would be 1500 pounds. Therefore, all of the hardware had to be rated to a safety factor of four at these given forces. By choosing 15-5 and 17-4 Stainless Steel as the materials for the design, this safety factor was reached.

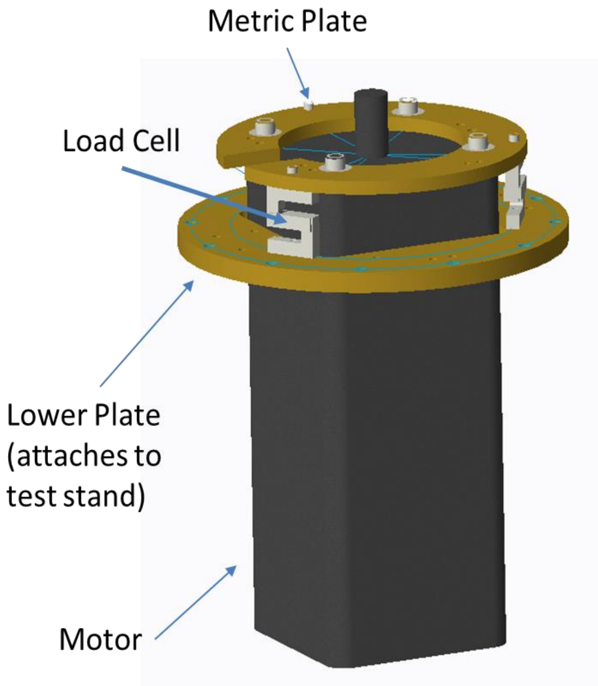

Figure 14: Siemens Motor Assembly

The design of the test stand also needed to be able to interface with the existing hardware that is used. The 40-inch propellers that are used as models of the actual 0.55 m Mars Scout Helicopter blades attach to a Siemens 1FT5102-5108 electric motor. The motor interfaces with several plates that are used to suspend the motor from whichever test stand it is attaching to. These plates also include load cells, which are used to gather data and measure forces.

In summary, the design specifications for the test stand were:

- Mount the rotor in a 0° configuration in the tunnel
- Mount the rotor in a 45° configuration in the tunnel (because of space)
- Include actuator hardware so that blades can be pitched remotely by +/- 10°
- Design hardware to withstand, with safety factor of 4, 1500 pounds of force in case of critical failure (blade breaks)

- Design hardware to interface with existing blades and motor

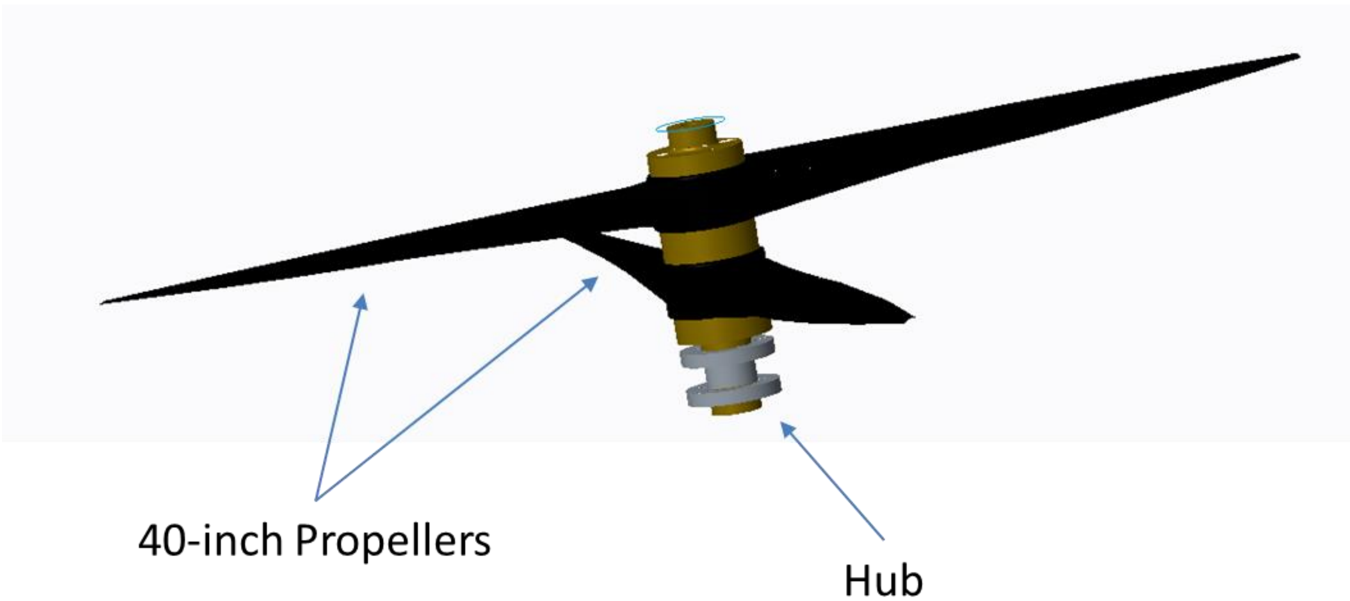

Figure 15: Blades and Hub

Concept Generation

Once the design specifications were explicitly stated and recorded, the concept generation process was begun. Initially, a stand was to be designed that would insert the rotor into the wind tunnel from the side. This stand would have had to bend at a 90° angle. While possible, this design concept was decided against ultimately because the blades would not have fit in the tunnel in this configuration. The tunnel is only 38 inches tall, while the blades are 40 inches in diameter. This design would also have been

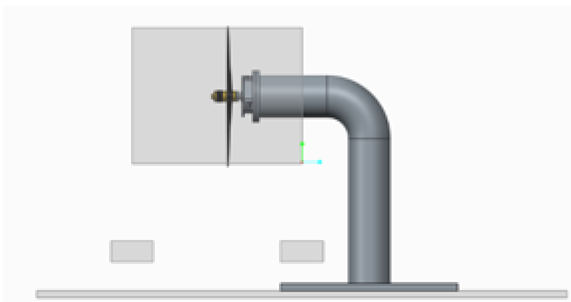

Figure 17: Concept 1

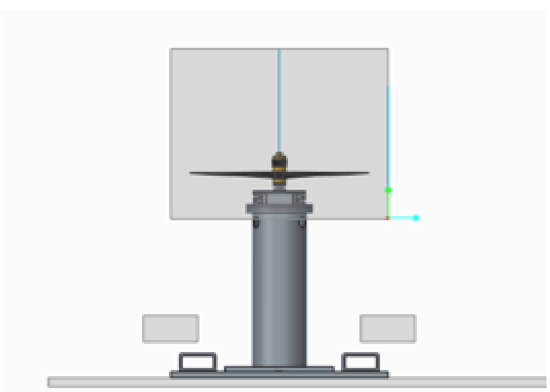

Figure 16: Concept 2

quite complicated. It would have been easy to tip, and also very unwieldy and heavy. In addition, it would not have been very portable.

The second concept that was considered was to insert the blades from the bottom of the tunnel. This design would basically have been a smaller version of the Hover Stand that was used at JPL.

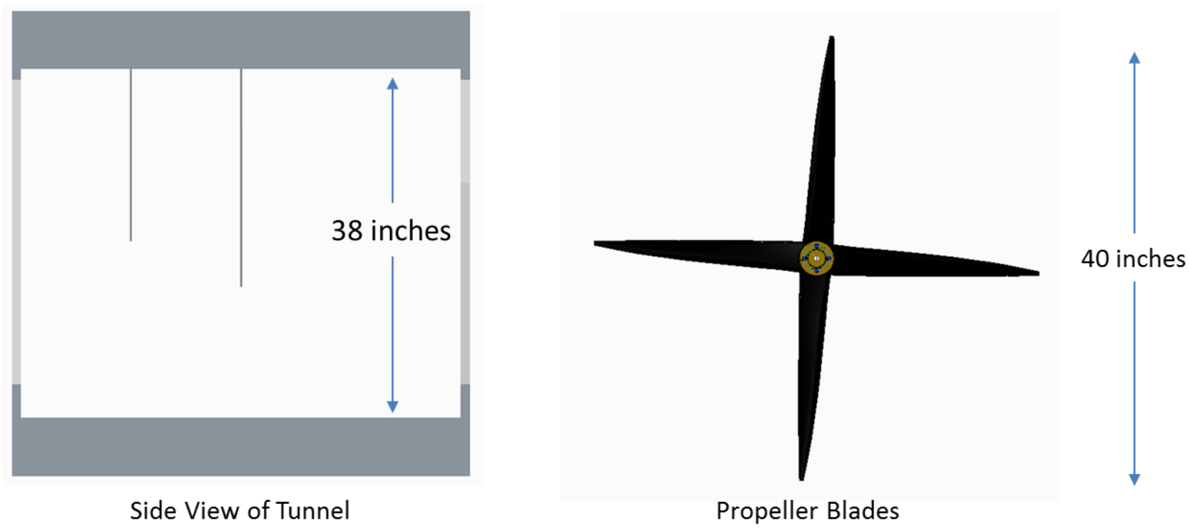

Figure 19: Tunnel and Propeller Comparison

Ultimately, this design was a step in the right direction, but was not as sophisticated as we were looking for. Pitching the blades in this configuration would have presented a challenge. In addition, the base plate that is used for the previously tested hover stand weighs 1000 pounds, while the tube portion of the stand weighs 700 pounds. Even scaled down, a test stand modeled after the hover stand would be very heavy and bulky. It would be difficult to position in the tunnel, as the tunnel is not mobile and is located in a tight space where forklifts do not have access.

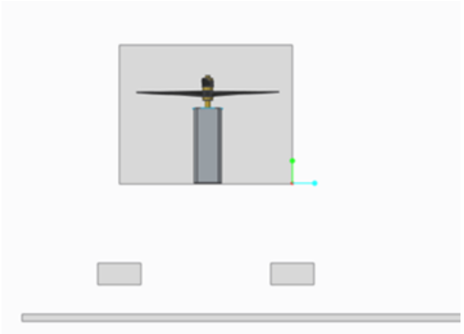
Figure 20: Motor in Tunnel Without Stand

In considering design options, the next logical step was to consider putting the stand inside the tunnel. Because the motor is so tall in and of itself, and because the ideal location for the blades in terms of flow quality is at the center of the tunnel, a good bit of time was spent discussing options which would allow a test stand to be placed inside the tunnel. Ultimately, it was decided that because the motor needs to be able to move with the blades and actuator, and because the rotor should be located at the center of the tunnel, the best option would be to suspend the motor through the floor of the tunnel. While this is not an option in many tunnels, the Mars Wind Tunnel has a plywood floor that the clients of the Wind Tunnel provide for their tests. Thus, suspending the motor through the floor is as easy as cutting a hole in the plywood.

Because the motor must be able to rotate, it was quickly evident that the motor would have to be suspended by a pin joint hinge. The design of these hinges evolved rapidly. The final design solution was to use screws to affix a pin component to the motor. This pin fit through a base piece that was bolted to a plate that bolts to the floor of the tunnel. A mounted ball bearing was fixed on the opposite side of the base piece from the pin to ensure smooth rotational motion.

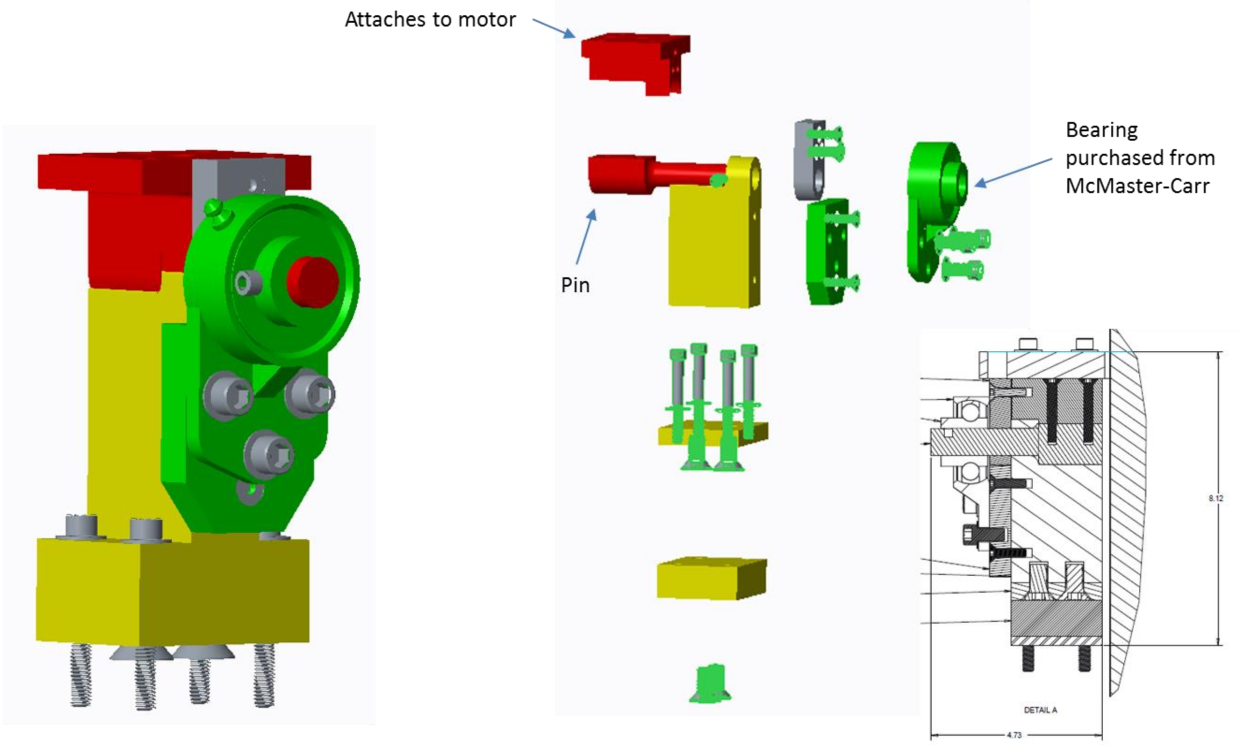

Figure 21: Hinge Design

Due to the high operating costs of the Aeolian Wind Tunnel, it was desirable to enable quick assembly and disassembly of both the 0° and 45° test modes. In order to accomplish this, the 0° stand was designed to attach directly to the 45° stand. For seamless interface, the pin and bearing assembly is bolted to a plate which is bolted to the tunnel floor for 0° mode. The actuator is also bolted to this plate. To convert to 45° mode, the plate is unbolted from the tunnel floor and bolted to the 45° stand. This reduces confusion during assembly, as there is minimal hardware and minimal hardware interchange.

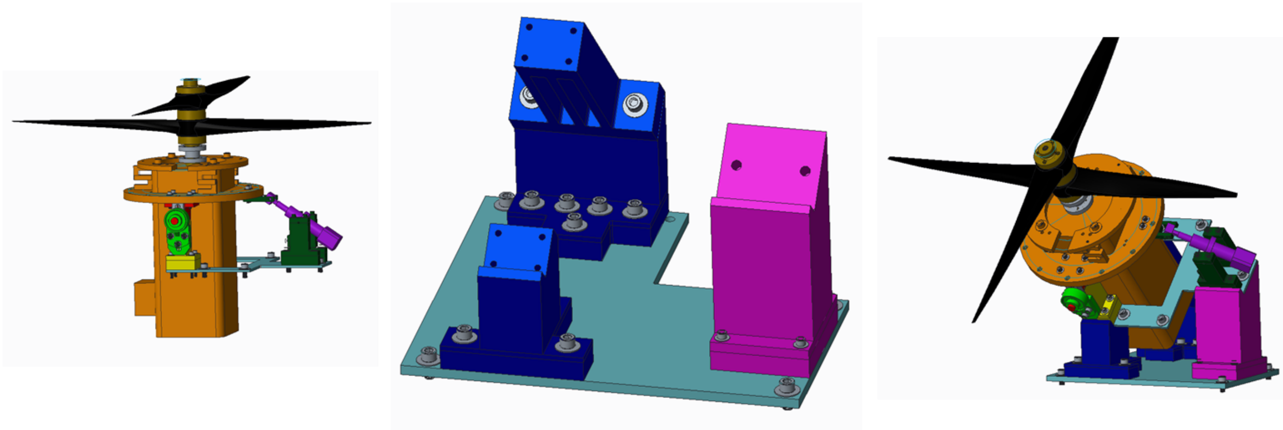

Figure 23: Interface Between 0° Mode and 45° Mode

Initially, the 45° stand was made up of one large piece of hardware that would have been unwieldy and very difficult to manufacture. After several design iterations, and after talking to the machine shop, the design of the 45° stand was modified for manufacturability. It was broken into three pieces, and then these three pieces were further simplified.

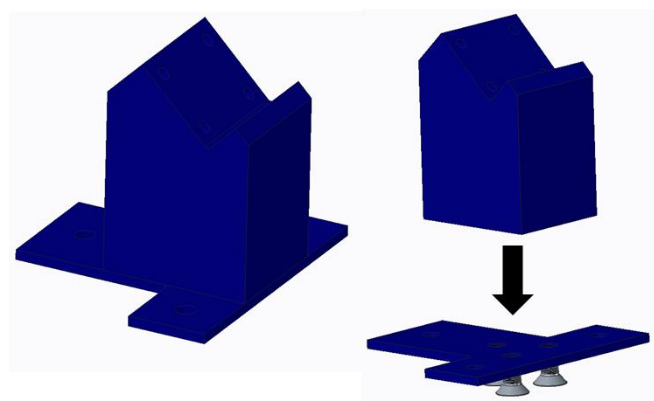

Figure 22: Design for Machinability

Ultimately, one of the design goals became to have a majority of the manufactured pieces be simple block shapes. This was largely accomplished, as only 4 out of the 30 components had a complicated geometry. The machine shop recommended that components such as the one depicted in Figure 22 be broken into two pieces and bolted together. This saves time in terms of machining, and also reduces that amount of material that is wasted in the machining process.After the simplification process, the components only required a few cuts in order to be machined. In addition, the components no longer required a weld. The components became easily storable and transportable because they can be completely disassembled.

The actuator stand was designed so that the actuator could have full range of rotation. The actuator was attached to the motor at a distance that would allow the motor to pitch a maximum of 10° forwards and backwards. Because the stand allows full range of motion, the actuator could be attached closer to the motor, which would allow a larger range of pitch rotation. The actuator itself is able to actuate 2 inches. In Figure 24, the actuator distance can be seen to be side *a*. Angle A is the required angle, which is 10° in each direction for a total of 20°. If *a* and A are known, the length of side *b* can be caluclated by:

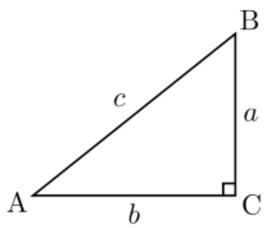

Figure 24: Calculate Actuator Placement

$$\tan(A) = \frac{a}{b}$$

Equation 3

$$b = \frac{a}{\tan(A)}$$

Equation 4

Since A = 20° and *a* = 2 inches, the length of side *b* is calculated to be 5.5 inches. Thus, the actuator was placed 5.5 inches away from the point of rotation.

The 0° stand and the 45° stand were designed to interface together seamlessly. Because the actuator had to be attached 5.5 inches away from the point of rotation, the actuator stand is slightly removed from the rest of the assembly. Because of this, when the stand is rotated to the 45° mode, there will be a large moment on the base plate where the actuator sits. Therefore, an actuator support was needed that attaches underneath the 0° base plate. This ensures that the actuator will be stable as it actuates and rotates the motor and blades.

Concept Evaluation

After the final design concept was completed, there were several iterations of design reviews and evaluations. The first few iterations focused on whether the design would work solely based on logic. The next design iterations focused on machinability, and to get a better perspective, initial drawings were taken to the machine shop. The machine shop managers looked over the design and provided feedback based on their knowledge of machines and materials. Because of their feedback, the design became much simpler and straight forward.

The final round of concept evaluation was completed regarding safety. As was previously mentioned, the force on the components of the stand at critical failure would be 1500 pounds. This force would be distributed through the components of the test stand. Each of the components was required to have a safety factor of four for the distributed force that it would feel at critical failure. For proof of safety, all of the analysis was run on individual components, and the force that was applied was assumed to be 1500 pounds. In addition, the direction of that 1500 pound force would vary based on what azimuth the blade breaks at. Because of this, in the FEA analysis, the force is applied along the axes of the components, as this constitutes the worst case scenarios. Most of the components were found to have a safety factor well over 4, even in these worst case scenarios. The components that did not have a safety factor of 4 were closely examined to determine how to increase the safety factor.

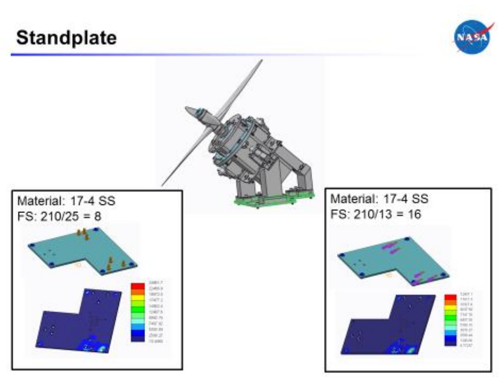

Figure 25: Standplate Analysis

One component that did not have a high enough safety factor was the 45° configuration base plate. Originally, the safety factor was less than 2. This was obviously unacceptable, so the plate was more closely examined to determine how to resolve this. The plate was originally only 0.25 inches thick. After increasing the thickness of the plate to 0.5 inches, the safety factor increased to 8. The full safety analysis ca be found in the appendix.

FS - Shearing of Bolts (worst case scenario of 2 bolts assumed)	
FS - Shearing of Set Screws (0.25 in diameter)	
Fmax (lb)	1500
Fmax/2-bolts (lb)	750
Area, A (in^2)	0.049087385
$Sigma_s$ = F/A (lb/in^2)	15278.87454
Shear Strength A-36 Steel Bolts	72000
FS	4.71238898
FS - Shearing of Set Screws (0.3125 in diameter)	
Fmax (lb)	1500
Fmax/2-bolts (lb)	750
Area, A (in^2)	0.076699039
$Sigma_s$ = F/A (lb/in^2)	9778.479704
Shear Strength A-36 Steel Bolts	72000
FS	7.363107782
FS - Shearing of Set Screws (0.375 in diameter)	
Fmax (lb)	1500
Fmax/2-bolts (lb)	750
Area, A (in^2)	0.110446617
$Sigma_s$ = F/A (lb/in^2)	6790.610905
Shear Strength A-36 Steel Bolts	72000
FS	10.60287521
FS - Shearing of Set Screws (0.5 in diameter)	
Fmax (lb)	1500
Fmax/2-bolts (lb)	750
Area, A (in^2)	0.196349541
$Sigma_s$ = F/A (lb/in^2)	3819.718634
Shear Strength A-36 Steel Bolts	72000
FS	18.84955592

Figure 26: Bolt Shear Analysis

These safety analysis procedures were followed for each component with an insufficient safety factor. For one component, it was necessary to increase the number of bolts securing it to its base. After adding one bolt, the safety factor increased to an acceptable range. In addition to the FEA analysis, it was also necessary to perform shear analysis on the bolts. The lowest ultimate strength of any bolt was 120 KSI, and the smallest diameter of any bolt was 0.25 inches. Again, the max force was taken to be 1500 pounds, as this would be realized at critical failure. As can be seen by the analysis in Figure 26, the safety factor is sufficient and there is no cause for concern. There is no valid fear that the bolts will shear and break.

Complete drawings were completed for this design iteration and can be found in the appendix.

Cost analysis

The largest cost for the project is the machining of the metal components. Because the on-site NASA machine shops can be utilized for all machining needs, it is easy to schedule a meeting with the shop supervisors to discuss the exact machining needs for each component in any design. This ensures that the work done is to the quality specifications necessary for the project. The shop does, however, charge more than an independent shop would charge. With that being said, we are currently waiting to hear back from the shop regarding an estimate for how many man hours it will take to machine all of the components. In addition to the machining costs, there is also a cost associated with the hardware that is necessary to assemble all of the components. The most costly item on the hardware parts list were the ball bearings, which were nearly $60.00 each. In total, the hardware costs came out to $276.63. There are a total of 160 assembly hardware components needed. Since McMaster sells screws and washers in packages, the total number of components that will be purchased is 437.

Item	Website	Part Num	Total	Come in Pa	Our Quant	Cost Each Pa	Cost
1/4-20, .625" HD Cap	http://www.mcmaster.com/#91274a160/=12b7ap5	91274A160	4	50	1	8.93	8.93
316 St-St Clevis Pin	http://www.mcmaster.com/#92401a643/=12b7azg	92401A643	1	5	1	12.81	12.81
316 St-St Washer .375"	http://www.mcmaster.com/#90107a127/=12b7b4i	90107A127	6	25	1	8	8
316 St-St Washer .3125"	http://www.mcmaster.com/#90107a030/=12b7ag5	90107A030	32	100	1	11.18	11.18
316 St-St Washer .5"	http://www.mcmaster.com/#90107a033/=12b7bat	90107A033	10	25	1	9.71	9.71
316 St-St Lock Washer .5"	http://www.mcmaster.com/#92147a033/=12b7cae	92147A033	11	25	1	6.44	6.44
0.375-24, .75" Socket	http://www.mcmaster.com/#90128a362/=12b7com	90128A362	6	25	1	11.76	11.76
.3125-18, 2.5" SOCKET	http://www.mcmaster.com/#91274a268/=12b7cwd	91274A268	8	10	1	6.92	6.92
.3125-18, 1.5" Socket	http://www.mcmaster.com/#91274a252/=12b7d5z	91274A252	14	25	1	9.36	9.36
.3125-18, 1.25" Socket	http://www.mcmaster.com/#91251a585/=12b7df1	91251A585	10	50	1	11.33	11.33
.25-20, 1.75" Flat	http://www.mcmaster.com/#91263a565/=12b7doa	91263A565	4	25	1	7.34	7.34
.25-20, 1.0" Flat	http://www.mcmaster.com/#91263a562/=12b7dxi	91263A562	14	25	1	8.59	8.59
.5-20, 1.0" Flat	http://www.mcmaster.com/#91263a795/=12b7e4o	91263A795	26	5	6	4.32	25.92
.5-20, 2.5" Socket	http://www.mcmaster.com/#90128a852/=12b7ejs	90128A852	2	5	1	8.52	8.52
.5-20, 1.0" Socket	http://www.mcmaster.com/#90128a840/=12b7eue	90128A840	10	5	2	5.2	10.4
Flange Mounted Ball Bearing, .75" Shaft Diameter	http://www.mcmaster.com/#8260k11/=12b7fs8	8260K110	2	1	2	59.71	119.4
Total Cost	**276.63**						

Figure 27: Test Stand Purchase List

Chapter 4

Discussion

As testing continues for the Mars Scout Helicopter, excitement will continue to build around the Mars 2020 rover mission. Larry Young and others of the Rotorcraft Aeromechanics branch have had a vision and a test plan to send a helicopter to Mars since the early 2000s. The involvement of JPL and the blessing of NASA headquarters is contributing to the success of what will become the first vehicle to fly on Mars. Since data was captured for the rotor in hover in December of 2015, new design tasks have been distributed, and new data collection tests have been commissioned. The forward flight test that is to be completed in the Ames Mars Aeolian Wind Tunnel is one of these data collection tasks, and will be the first test to gather such data. By gathering data on rotor performance in terms of thrust, torque and power in a forward flight configuration under Martian conditions, NASA scientists and engineers will be able to more accurately address the challenges of flying a helicopter on Mars. Further, with the remotely controlled actuator that will pitch the blades both 10° into the wind as well as 10° out of the wind, data can also be gathered for what could be considered landing conditions.

The Mars Aeolian Wind Tunnel is generally used to test the behavior of the Martian dust and dirt when it is exposed to Martian winds. Because the tunnel already has the capability to deal with such dust particles, testing is also possible for rotor performance with interference from Martian winds and dust. This will allow for even more in depth testing and data collection.

Conclusion

Within this design task there were many details that were combed through that are not mentioned in this report in order to avoid monotony as well as to prevent the length of the report from becoming excessive.

The main objective of this project was to design a test stand to be used in the Mars Aeolian Wind Tunnel. The stand was to be able to interface with the existing hardware, including the 40-inch propellers and the Siemens Electric Motor. In addition, the stand was to include two configurations, namely a 0° configuration, where the rotor blades were parallel to the wind tunnel floor, and a 45° configuration, where the rotor blades were to be at a 45° angle relative to the tunnel floor. These two configurations were to interface together in such a way to reduce machining time, as well as reduce assembly set-up and disassembly times. The design was also required to allow the motor and blades to be pitched 10° into and out of the wind. In order to pitch the blades, an actuator was necessary, so the design was also to include interface for that actuator. Each component of the stand was to withstand the critical failure force of 1500 pounds, which would occur if a blade were to break during testing at 3000 RPM. These specifications were given by the engineers at Ames Research Center.

All of the previously stated design specifications were met with the design of the Mars Aeolian Wind Tunnel Test Stand. This stand will be used in May or June of 2016 to test rotor performance in forward flight in a reduced pressure, Martian-like environment. No comparable test has, as of yet, been completed, so this test will mark a new era in vehicle flight testing in atmospheres other than that of earth.

References

AKSteel. (2007). *15-5 PH Stainless Steel Data Sheet*. Retrieved from AKSteel.com: http://www.aksteel.com/pdf/markets_products/stainless/precipitation/15-5_ph_data_sheet.pdf

Chen, G. H. (2015). Computational and Experimental Studies Towards the Development of a Prototype Mars Rotorcraft and Data reduction of the Boeing SMART Rotor Full-Scale Wind Tunnel Test.

Young, L., Aiken, E., Derby, M., Demblewski, R., & Navarrete, J. (n.d.). Experimental Investigation and Demonstration of Rotary Wing for Flight in the Atmosphere of Mars.

Appendix

HUB SOP

Necessary Equipment:

- Hardware:
  - Hub Adapter x1
  - Lower Prop x1
  - Washer x1
  - Upper prop x1
  - Top Lock x1
  - Ringfeder Shrink Disc x1
  - 3/16 bolt x8
  - 3/8 bolt x1
- Tools:
  - Ratchet socket wrench x1
  - 3/16 socket key x1
  - 3/8 socket key x1
  - Calibrated torque wrench x1
  - Loctite 242 x1
  - Wire brush x1
  - Napkin/paper towel x2-3

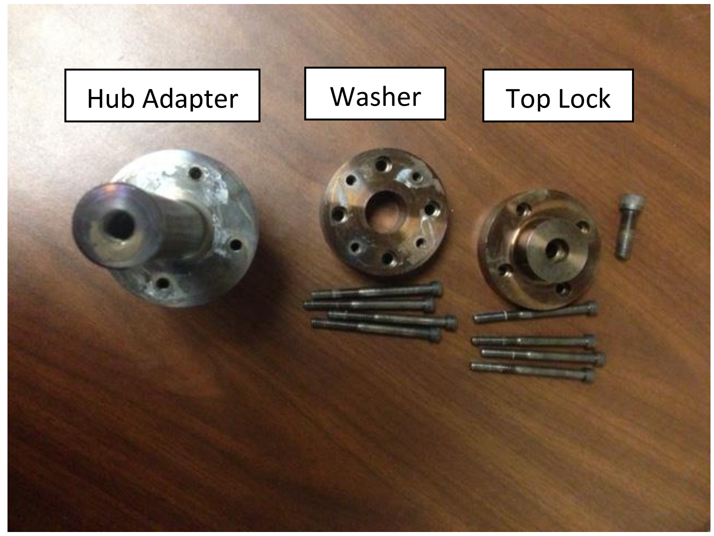

Wire Brush – Step 2

1. Practice using the calibrated torque wrench to tighten practice screws to 9 ft-lbs
2. Scrub leftover Loctite off of the 3/16” screws using the wire brush
3. Put the upper prop (screw holes at 45 degrees off main axes) on the hub adapter
4. Put washer on hub adapter (over upper prop)
5. Set calibrated torque wrench to 9 ft-lbs
6. Place Loctite on threads of first four 3/16” screws. Loctite should form fine layer on bottom three threads of screw
7. Place four 3/16” screws in washer and tighten. Torque to 9 ft-lbs (108 in-lbs) (practice using wrench first). Take care not to over-torque – this may cause stripping of the bolt head

Upper Prop – Step 3

8. Place the lower rotor (screws in line with major axes) on the hub adapter
9. Place top lock on top of lower rotor

Lower Prop – Step 8

10. Place Loctite on threads of last four 3/16” screws. Loctite should form fine layer on bottom three threads of screw
11. Place four 3/16” screws in top lock and tighten. Torque to 9 ft-lbs (108 in-lbs)
12. Place 3/8” screw in top of top lock and tighten. Torque to 31 ft-lbs (372 in-lbs)
13. Record date of assembly/disassembly on attached data sheet
14. After 10 assemblies, replace 3/16” screws and record the replacement

Mars Hub Stand Analysis

FS - Bending of Small Cylinder - Gravitational Force

Weight, Total of stand, (lb)	37.353
Weight, W Total of Stand, (kg)	16.958
Newtons to pounds conversion	4.448
6061 Aluminum (psi)	45000.000
Rod thickness, d (in)	1.125
Diameter	1.125
Area	0.994
Height	2.225
Volume (Cyl Structure)	67.300
Density (Al)	0.098
Volume (Base Plate)	109.970
Density (A36 Steel)	0.280
Weight	37.353

Gravitational Force (lb) F_g=m*g	Inertia I=Pi*d^4/64	M=f*Length	C=d/2	$Sigma_B$=M*C/I	Factor of Safety Aluminum 6061
37.400	0.079	83.214	0.563	595.306	75.591

FS - Stress Concentration Factor on Central 1.125" diameter shaft

F (lb) - From dropping mechanism	37.4
6061 Aluminum (psi)	45000
L = Length Rod (in)	2.225
Moment, M = F*L, (lb*in)	83.215
D, width of disk (in)	3
d, width of shaft (in)	1.125
c =d / 2, (in)	0.5625
I = Pi*d^4/64 (in^4)	0.0786285
r, fillet radius (in)	0.09
r / d	0.08
$Sigma_{AVG}$ = M*c/I	595.3113405
Average FS	75.59069841
K_t	1.8
$Sigma_{ACTUAL}$ = K_t*$Sigma_{AVG}$	1071.560413
Actual FS_{ACTUAL}	41.99483245

<< This is the fillet radius for 1.125" Hub shaft

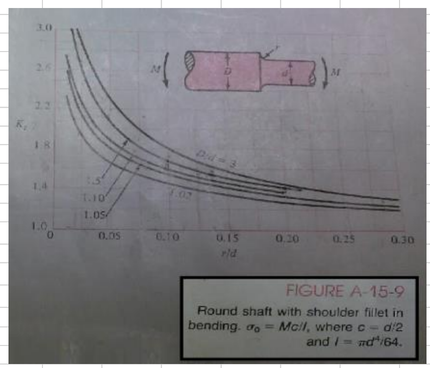

FIGURE A-15-9
Round shaft with shoulder fillet in bending. $\sigma_0 = Mc/I$, where $c = d/2$ and $I = \pi d^4/64$.

FS - Shearing of 3 Bolts from Max bending moment from dropping mechanism

FS - Bending Moment vs 4-Bolts	
Fmax (lb)	37.4
Fmax/4-bolts (lb)	9.35
Area, A (in^2)	0.110446617
$Sigma_s$ = F/A (lb/in^2)	84.65628262
Shear Strength A-36 Steel Bolts	34800
FS	411.0740387

Shear is 60% of the Tensile Strength. 58,000 psi Tensile --> .6*58,000 = 34,800 psi

http://www.portlandbolt.com/technical/faqs/bolt-shear-strength-considerations/

FS - Tipping Moment		(The center of gravity concidered is the worst case scenario at the top of the rotor hub assembly attached to the assembly base)
Total Weight	48	
Radius	7.5	
Y_{CoG}	18	<- This is the height of the Hardware and the rotor
M=Wt*R+F*Ycg=0		
F=Wt*R/Ycg		
Force Applied	20	
$\sigma = \tan^{-1}(F/Wt)$		
Critical Angle	22.61986	

Mars Hub Stand Drawings

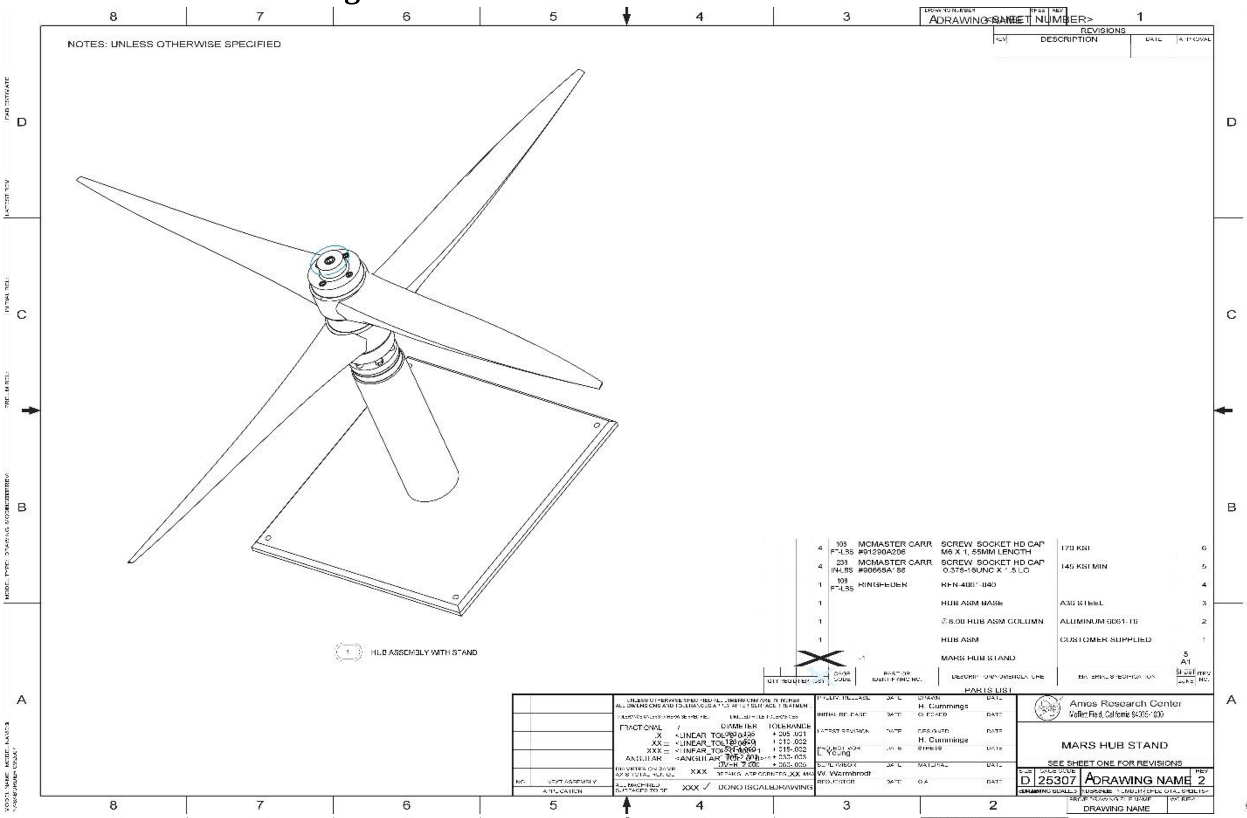

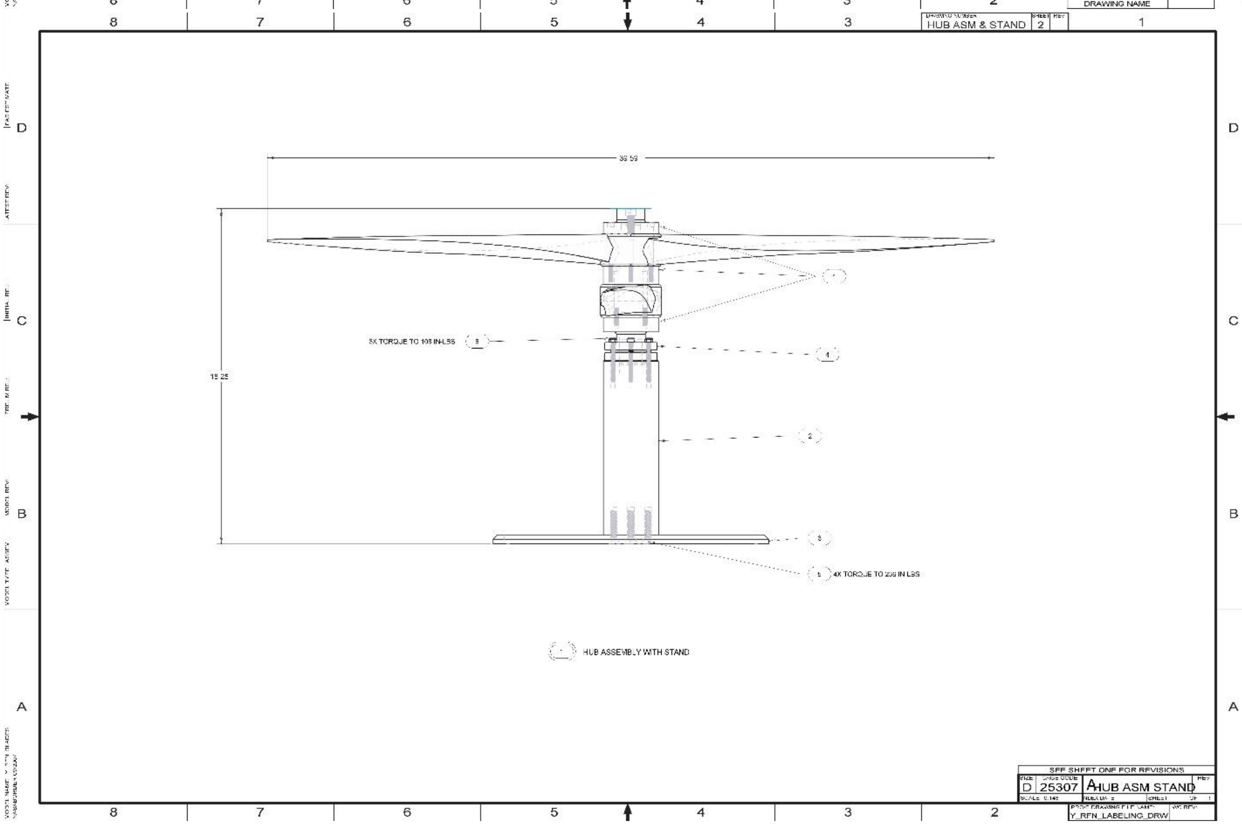

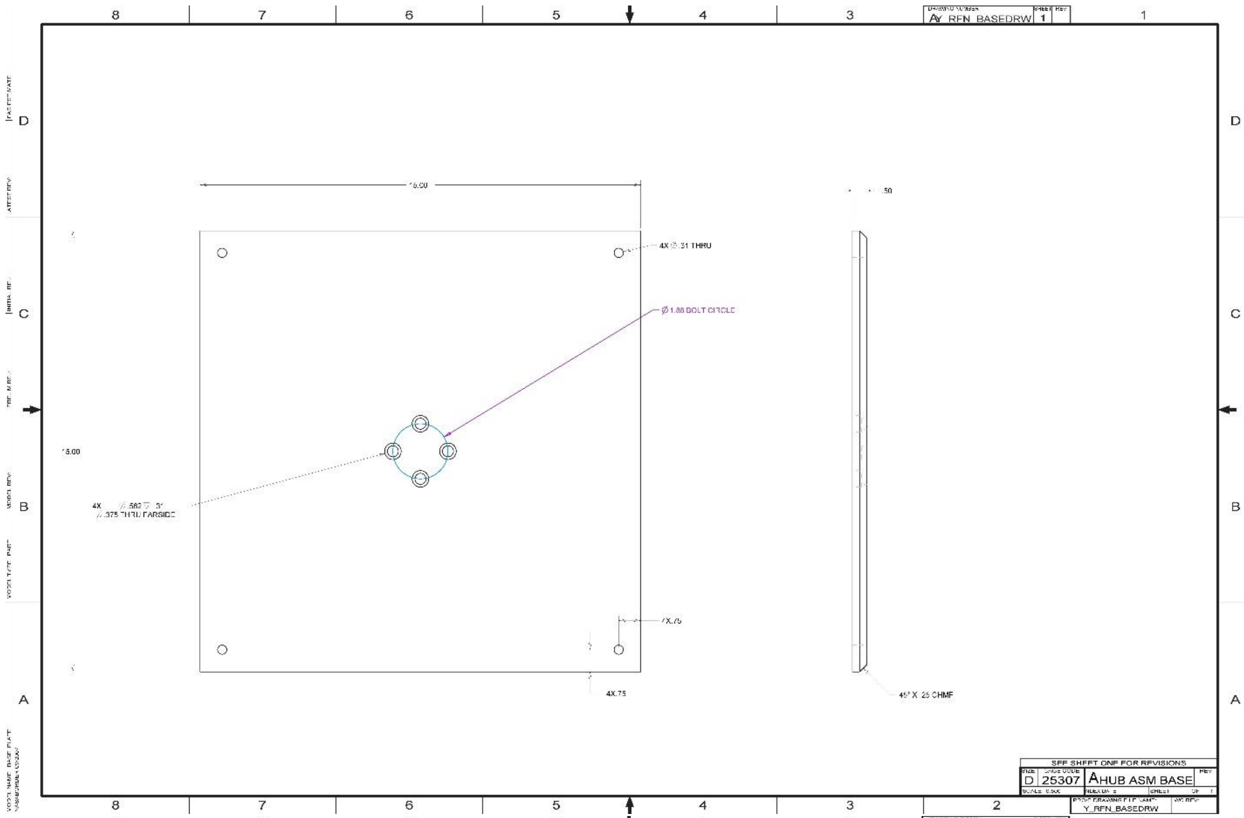
AY RFN_BASEDRW
16.00
.50
4X ⌀.31 THRU
⌀1.88 BOLT CIRCLE
16.00
4X.75
45° X .25 CHMF
SEE SHEET ONE FOR REVISIONS
D 25307 AHUB ASM BASE
Y_RFN_BASEDRW

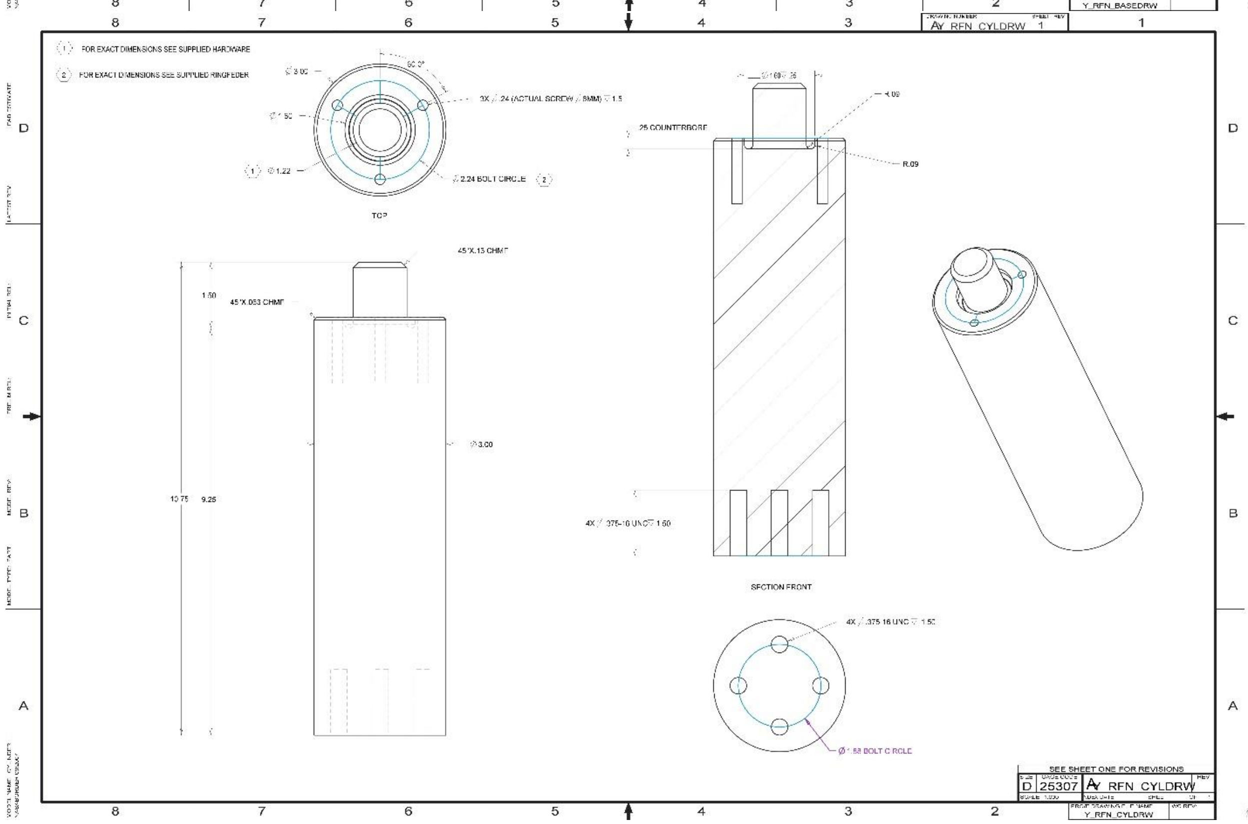
AY RFN_CYLDRW
FOR EXACT DIMENSIONS SEE SUPPLIED HARDWARE
FOR EXACT DIMENSIONS SEE SUPPLIED RINGFEDER
⌀3.00
⌀1.50
⌀1.22
⌀2.24 BOLT CIRCLE
TOP
45°X.13 CHMF
1.50
45°X.063 CHMF
⌀3.00
10.75
9.25
.25 COUNTERBORE
R.09
R.09
4X ⌀.375-16 UNC ▽ 1.50
SECTION FRONT
4X ⌀.375-16 UNC ▽ 1.50
⌀1.88 BOLT CIRCLE
SEE SHEET ONE FOR REVISIONS
D 25307 AY RFN_CYLDRW
Y_RFN_CYLDRW

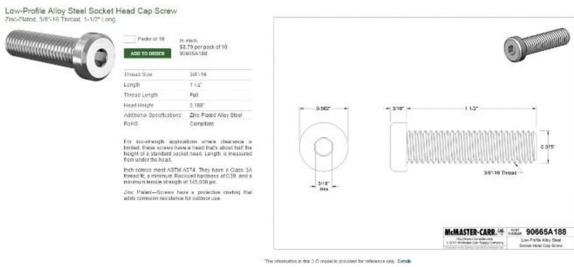

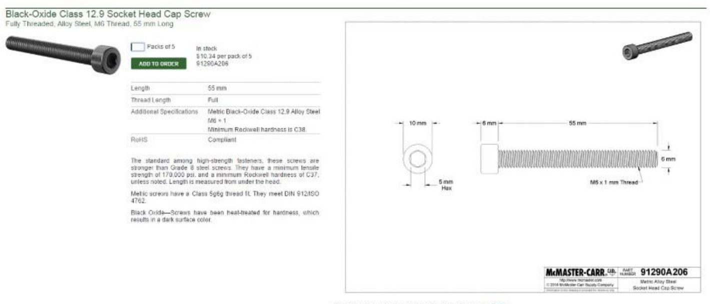

Item	Website	Part Num	Total	Come in Pac	Our Quanti	Cost Each Pac	Cost
Ringfeder RFN 4061-040	http://www.ringfeder.com/en/international/products/ringfeder/Product/?p=4803	RFN 4061-040	1	1	1	93.13	93.13
3/8-16, 1.5" Low-Profile Screw	http://www.mcmaster.com/#90665a188/=11e6v1x	90665A188	4	10	1	8.79	8.79
M6X55 Screw	http://www.mcmaster.com/#91290a206/=10yfrxy	91290A206	3	5	1	10.34	10.34
Adhesive back neoprene rubber	http://www.mcmaster.com/#1374n12/=10ye30s	1374N12	2	1	2	8.47	16.94

Total
129.2

Mars Aeolian Wind Tunnel Test Stand Analysis

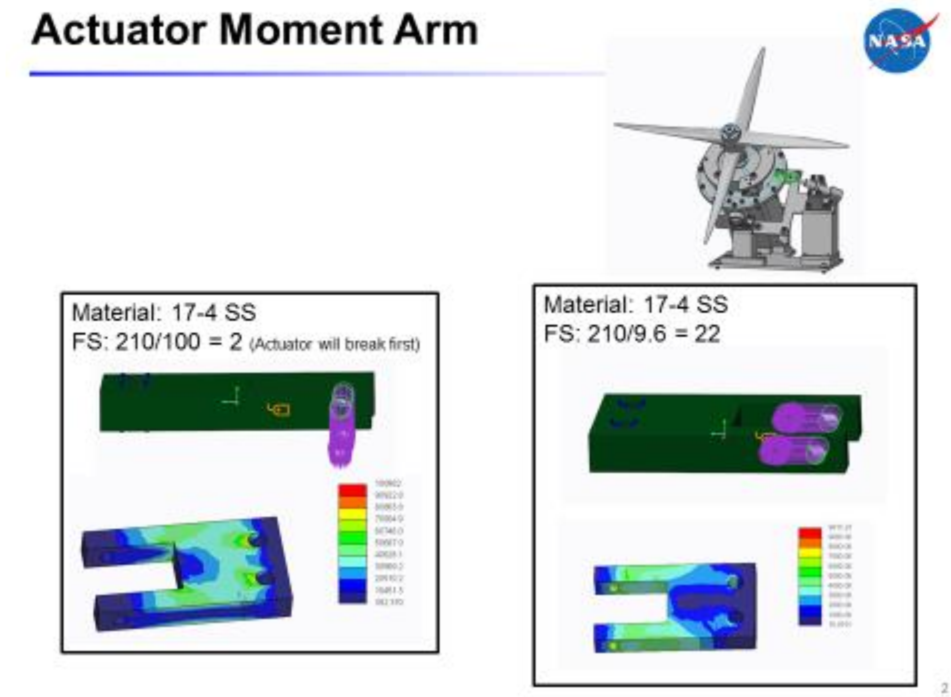

Actuator Pivot

Material: 17-4 SS
FS: 210/16 = 13

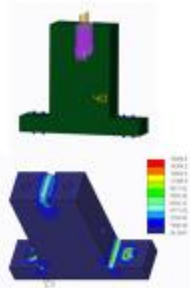

Material: 17-4 SS
FS: 210/152 = 1.4
(actuator will break first)

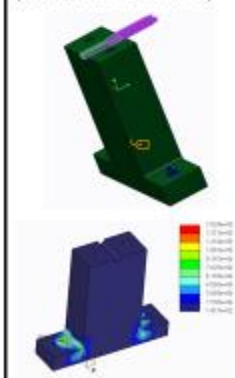

3

Actuator Rotator

Material: 17-4 SS
FS: 210/77 = 2.7 (actuator will break first)

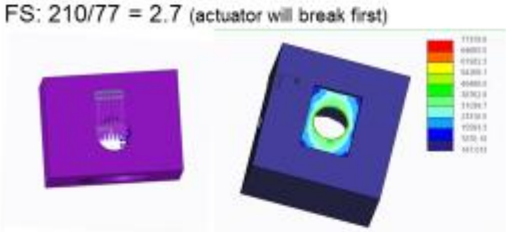

4

Actuator Base

Material: 17-4 SS
FS: 210/17 = 12

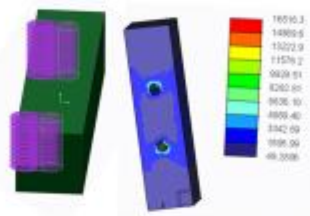

Material: 17-4 SS
FS: 210/16 = 13

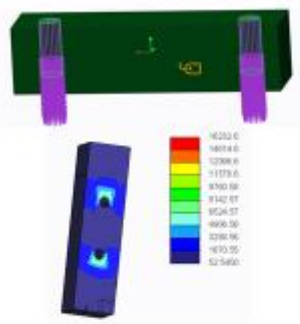

Pin Base

Material: 17-4 SS
FS: 210/41 = 5

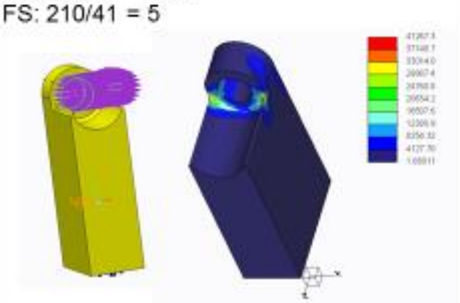

Material: 17-4 SS
FS: 210/41 = 5

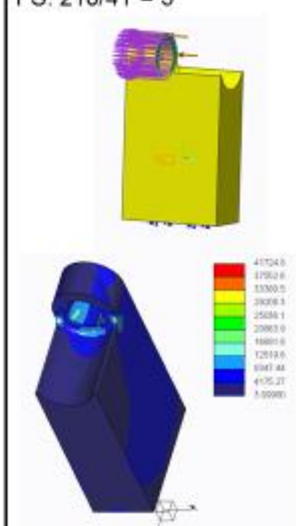

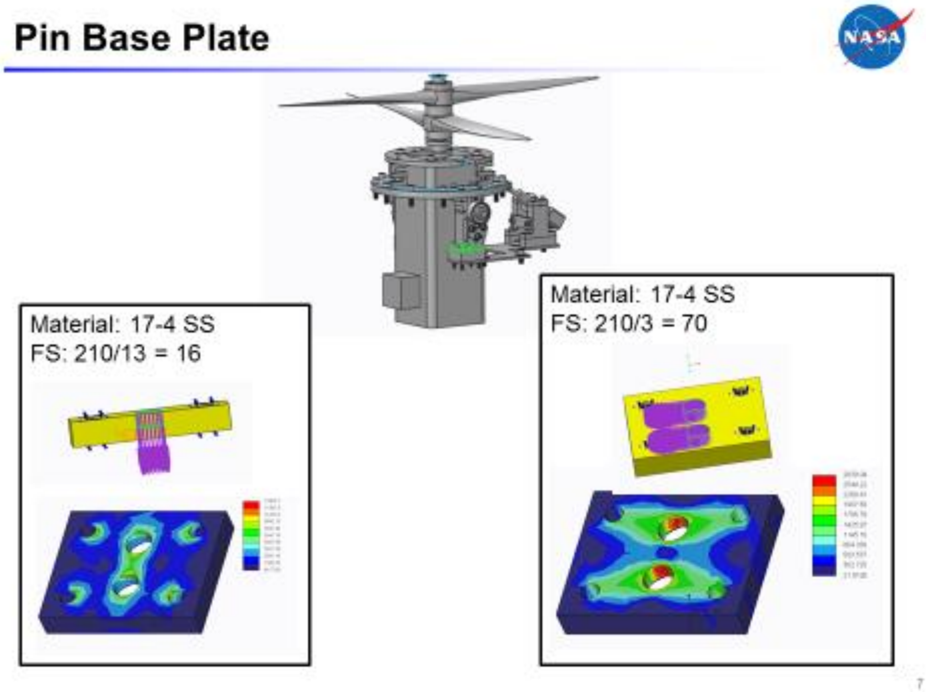
Pin Base Plate
Material: 17-4 SS
FS: 210/13 = 16
Material: 17-4 SS
FS: 210/3 = 70

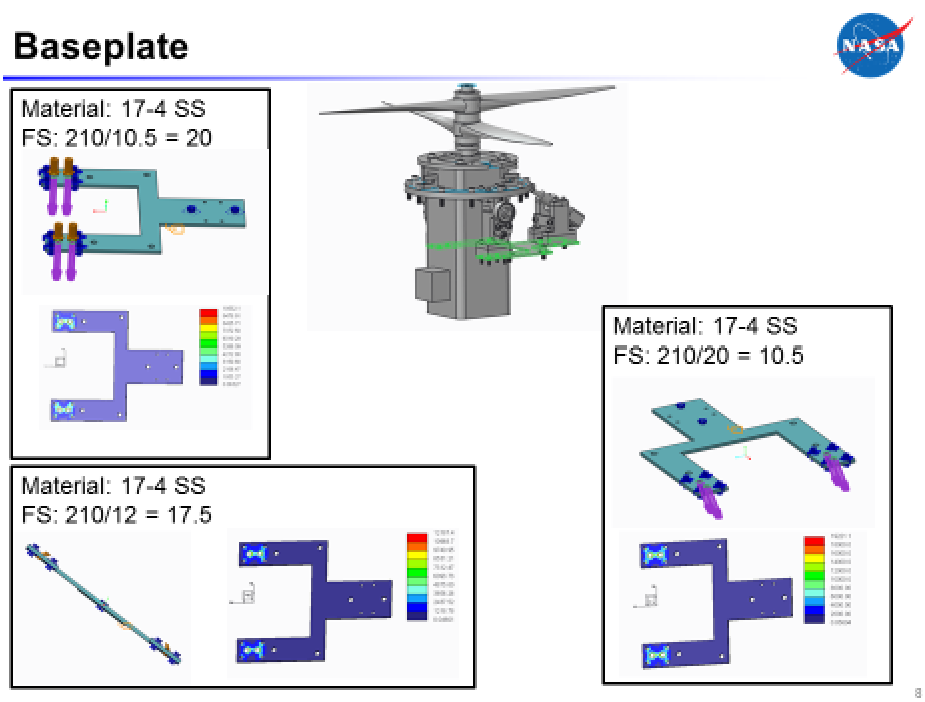
Baseplate
Material: 17-4 SS
FS: 210/10.5 = 20
Material: 17-4 SS
FS: 210/20 = 10.5
Material: 17-4 SS
FS: 210/12 = 17.5

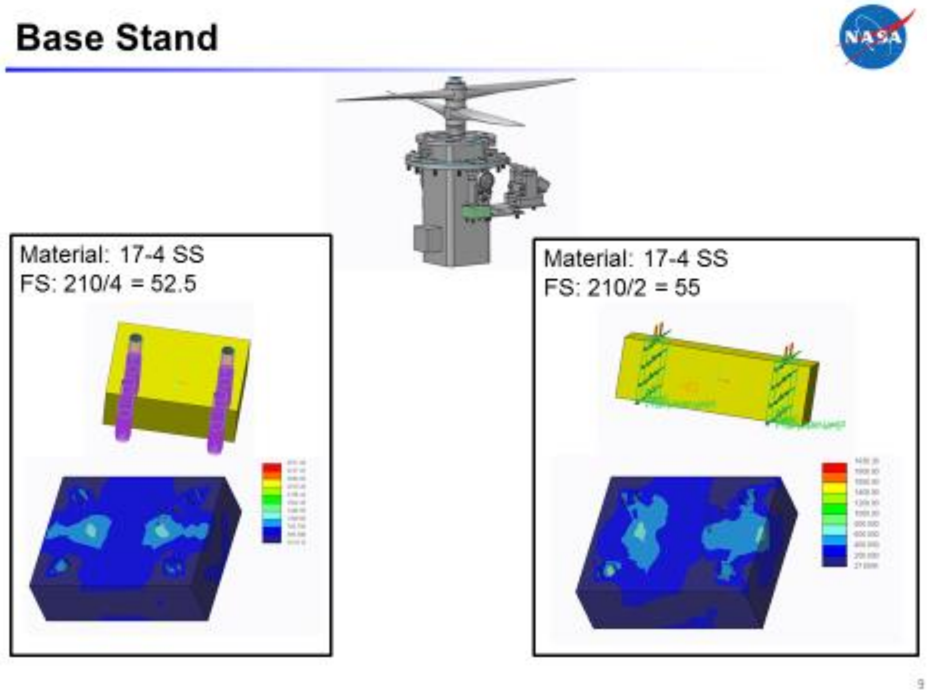
Base Stand
Material: 17-4 SS
FS: 210/4 = 52.5
Material: 17-4 SS
FS: 210/2 = 55
9

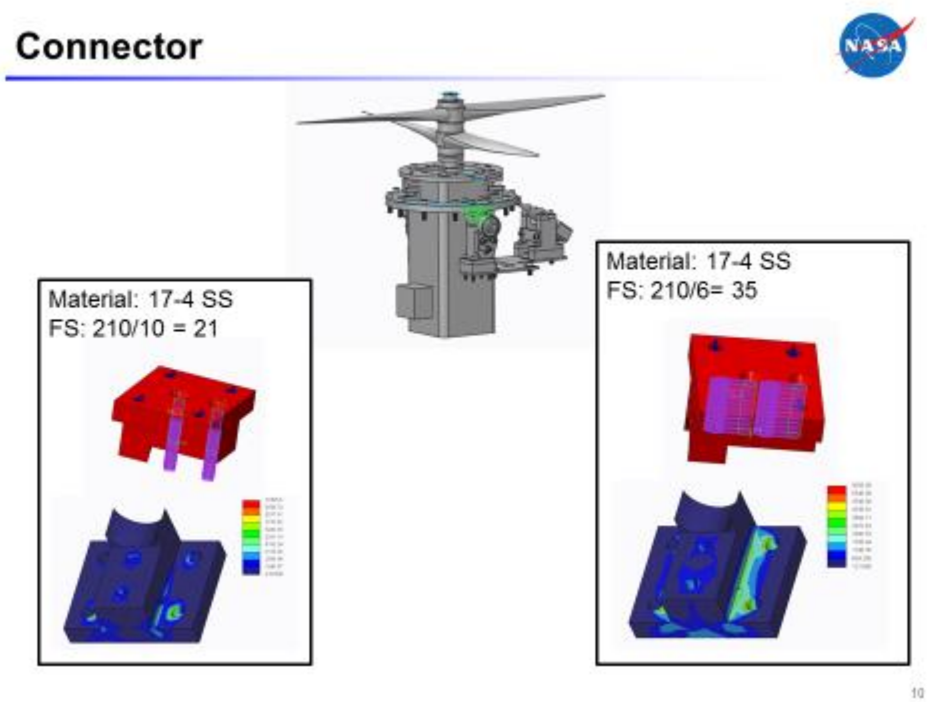
Connector
Material: 17-4 SS
FS: 210/10 = 21
Material: 17-4 SS
FS: 210/6= 35
10

45° Config Tower

Material: 17-4 SS
FS: 210/22 = 9

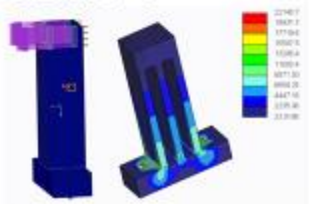

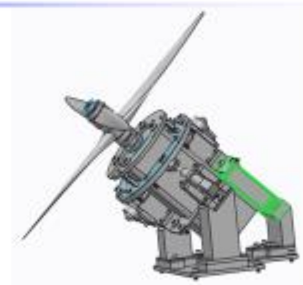

Material: 17-4 SS
FS: 210/3 = 70

Material: 17-4 SS
FS: 210/11 = 19

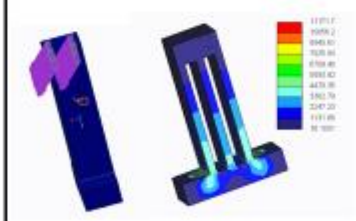

45° Config Front Support

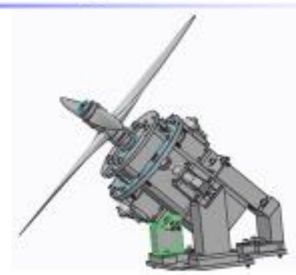

Material: 17-4 SS
FS: 210/3 = 70

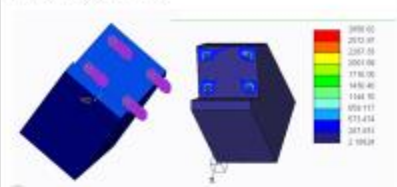

Material: 17-4 SS
FS: 210/7 = 30

Front Support Plate

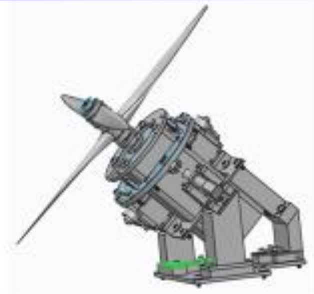

Material: 17-4 SS
FS: 210/43 = 5

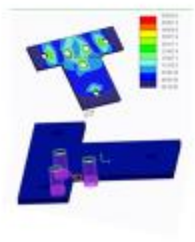

Material: 17-4 SS
FS: 210/15 = 14

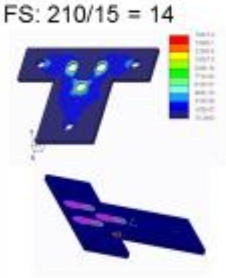

Tower Support

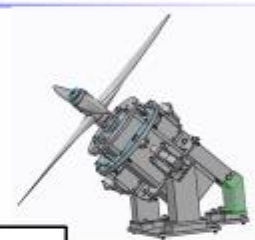

Material: 17-4 SS
FS: 210/2 = 105

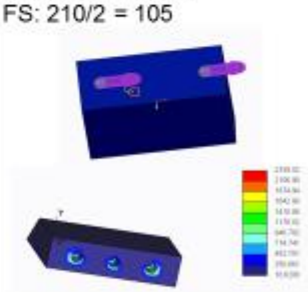

Material: 17-4 SS
FS: 210/3 = 70

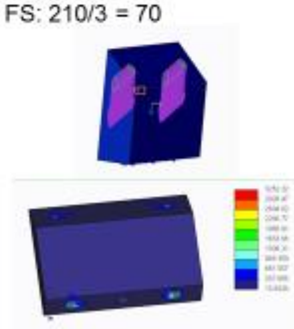

Tower Support Plate

Material: 17-4 SS
FS: 210/60 = 3.5

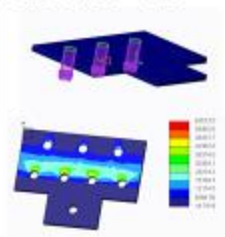

Material: 17-4 SS
FS: 210/14 = 15

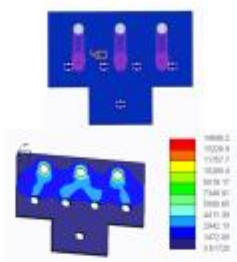

Support

Material: 17-4 SS
FS: 210/2 = 105

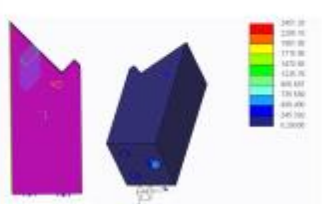

Material: 17-4 SS
FS: 210/8 = 26

Support Plate

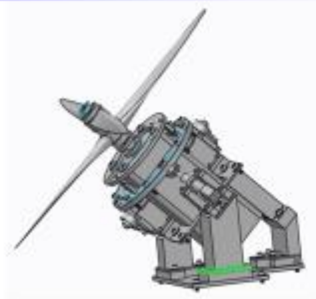

Material: 17-4 SS
FS: 210/3 = 70

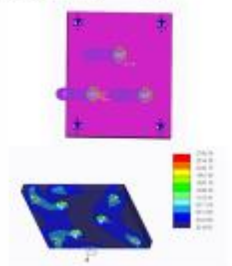

Material: 17-4 SS
FS: 210/19 = 11

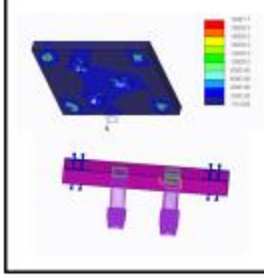

Support Stand

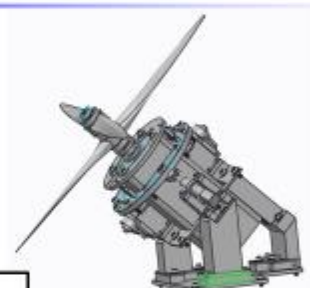

Material: 17-4 SS
FS: 210/5 = 42

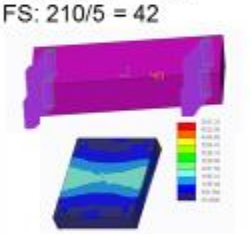

Material: 17-4 SS
FS: 210/2 = 105

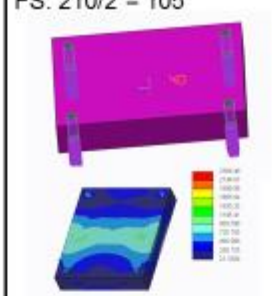

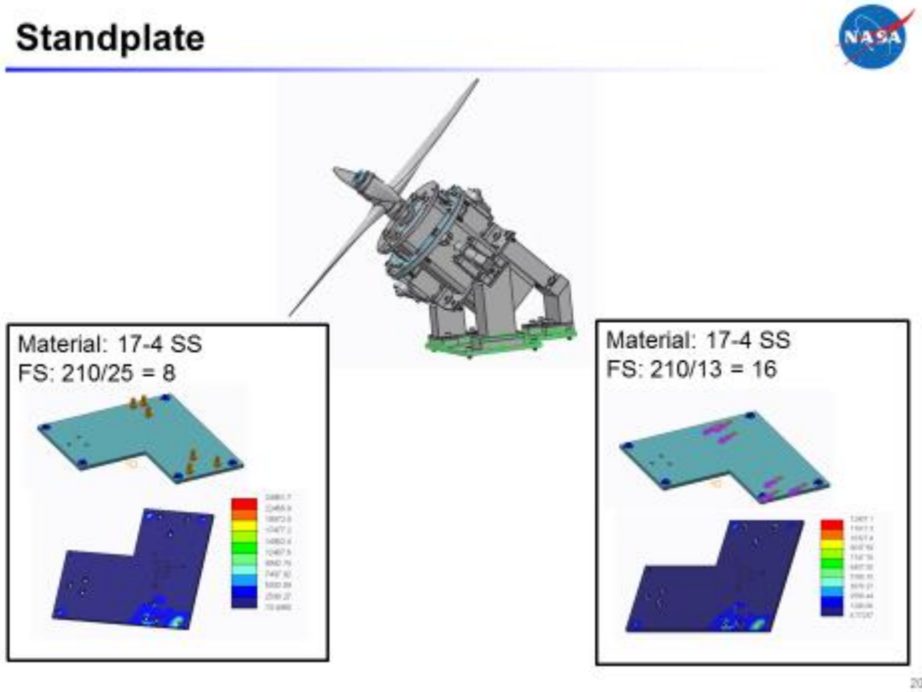
Standplate
Material: 17-4 SS
FS: 210/25 = 8
Material: 17-4 SS
FS: 210/13 = 16
20

Mars Aeolian Wind Tunnel Test Stand Engineering Drawings

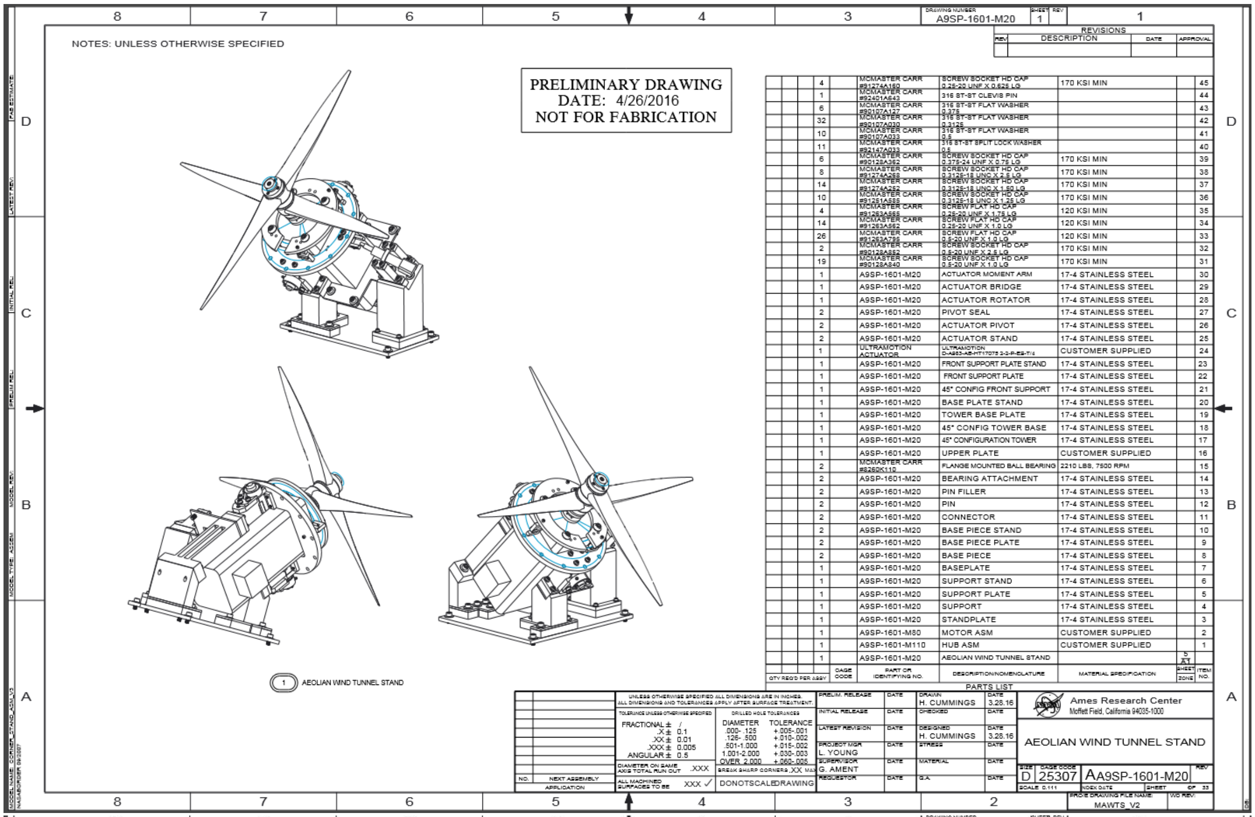

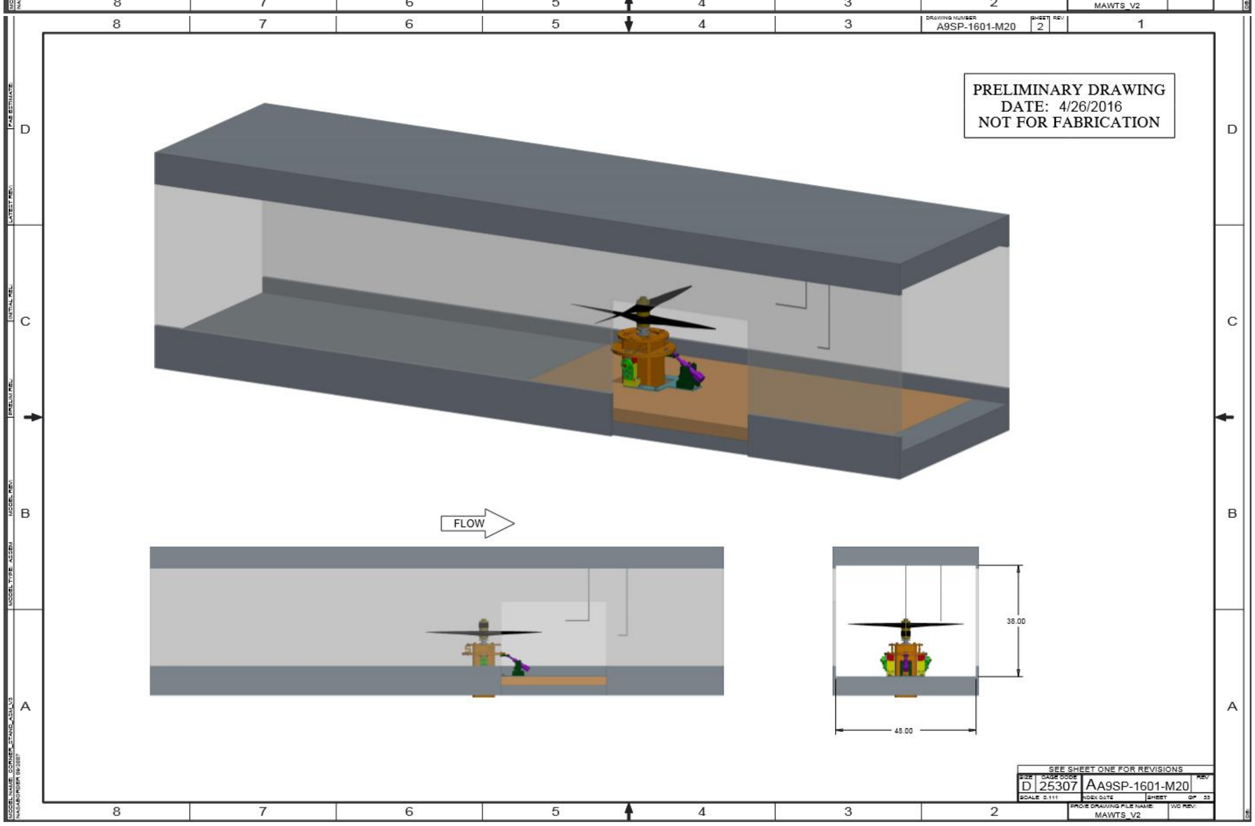

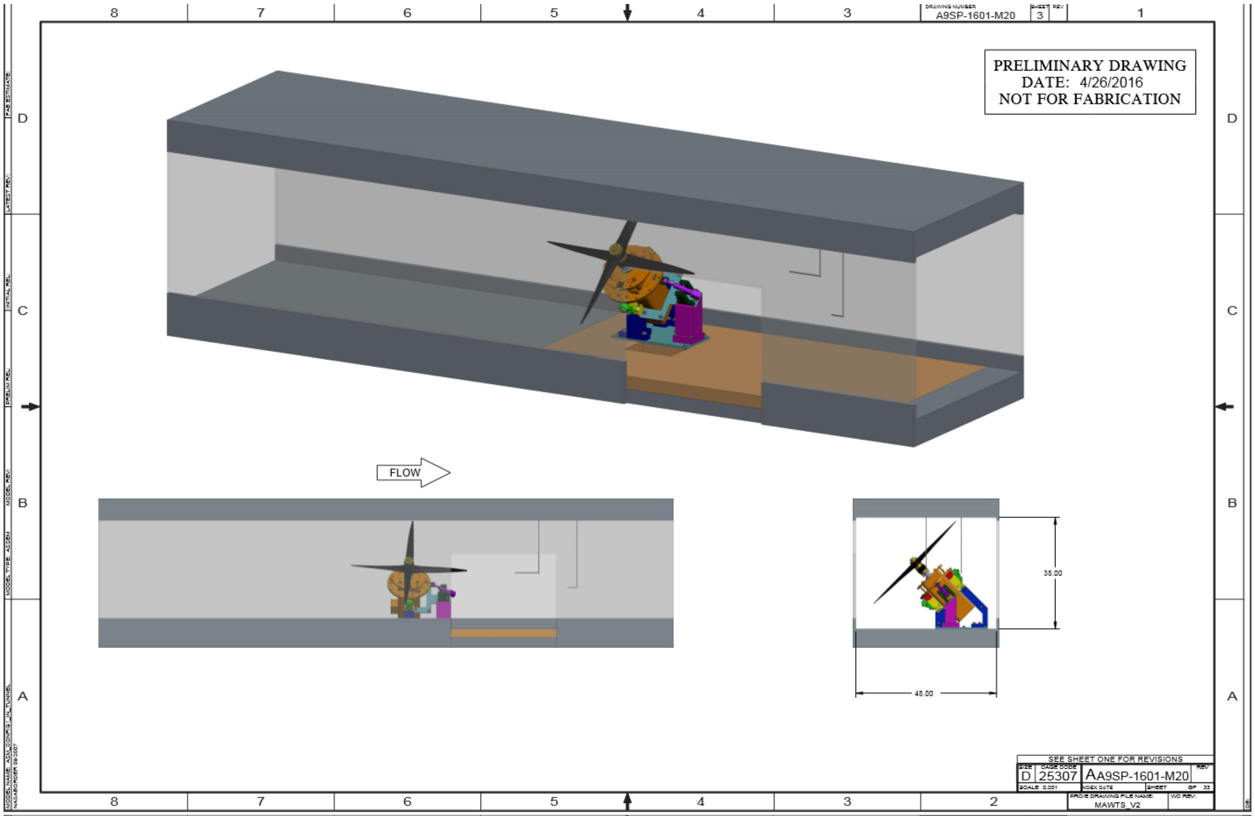
A9SP-1601-M20
3
PRELIMINARY DRAWING
DATE: 4/26/2016
NOT FOR FABRICATION
FLOW
38.00
48.00
SEE SHEET ONE FOR REVISIONS
D 25307 AA9SP-1601-M20
MAWTS_V2

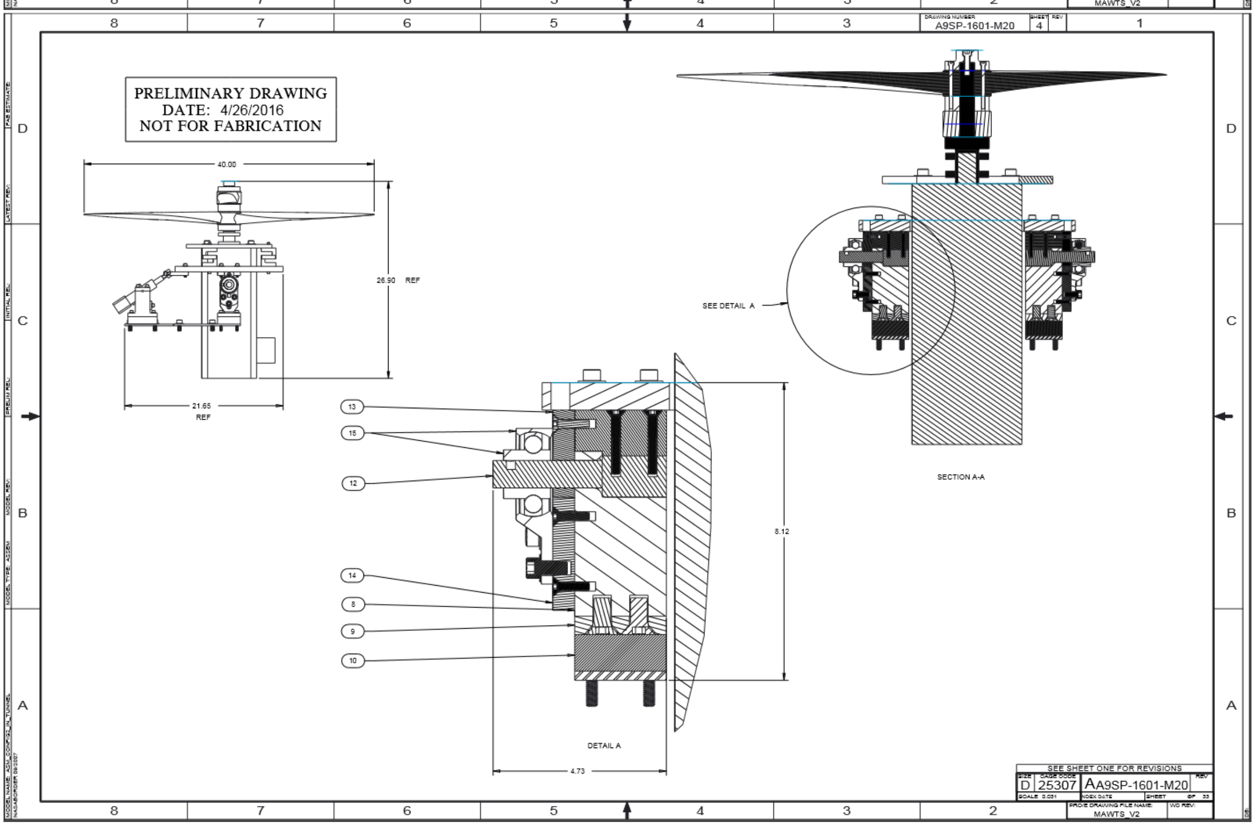
A9SP-1601-M20
4
PRELIMINARY DRAWING
DATE: 4/26/2016
NOT FOR FABRICATION
40.00
26.90 REF
21.65
REF
SEE DETAIL A
SECTION A-A
13
15
12
14
8
9
10
8.12
DETAIL A
4.73
SEE SHEET ONE FOR REVISIONS
D 25307 AA9SP-1601-M20
MAWTS_V2

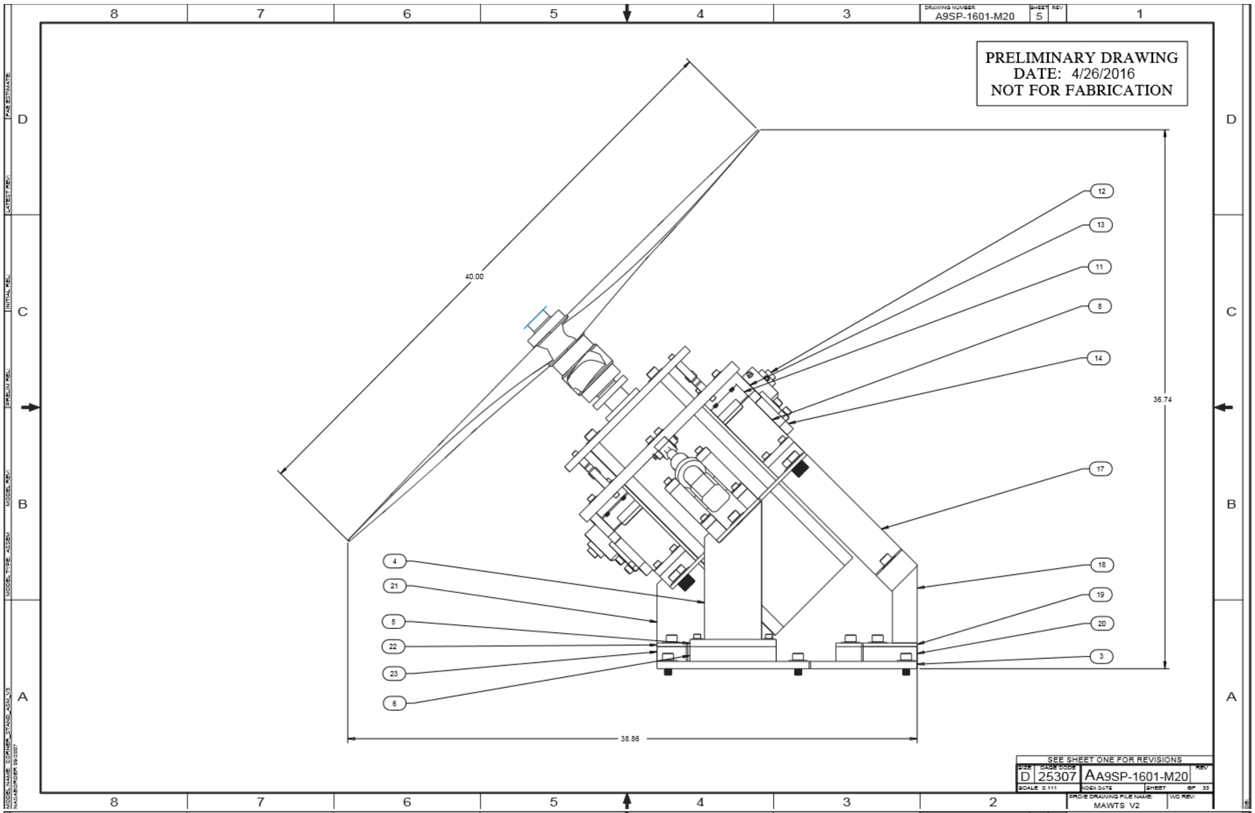
A9SP-1601-M20
PRELIMINARY DRAWING
DATE: 4/26/2016
NOT FOR FABRICATION
40.00
36.74
38.86
SEE SHEET ONE FOR REVISIONS
D 25307 AA9SP-1601-M20
MAWTS V2

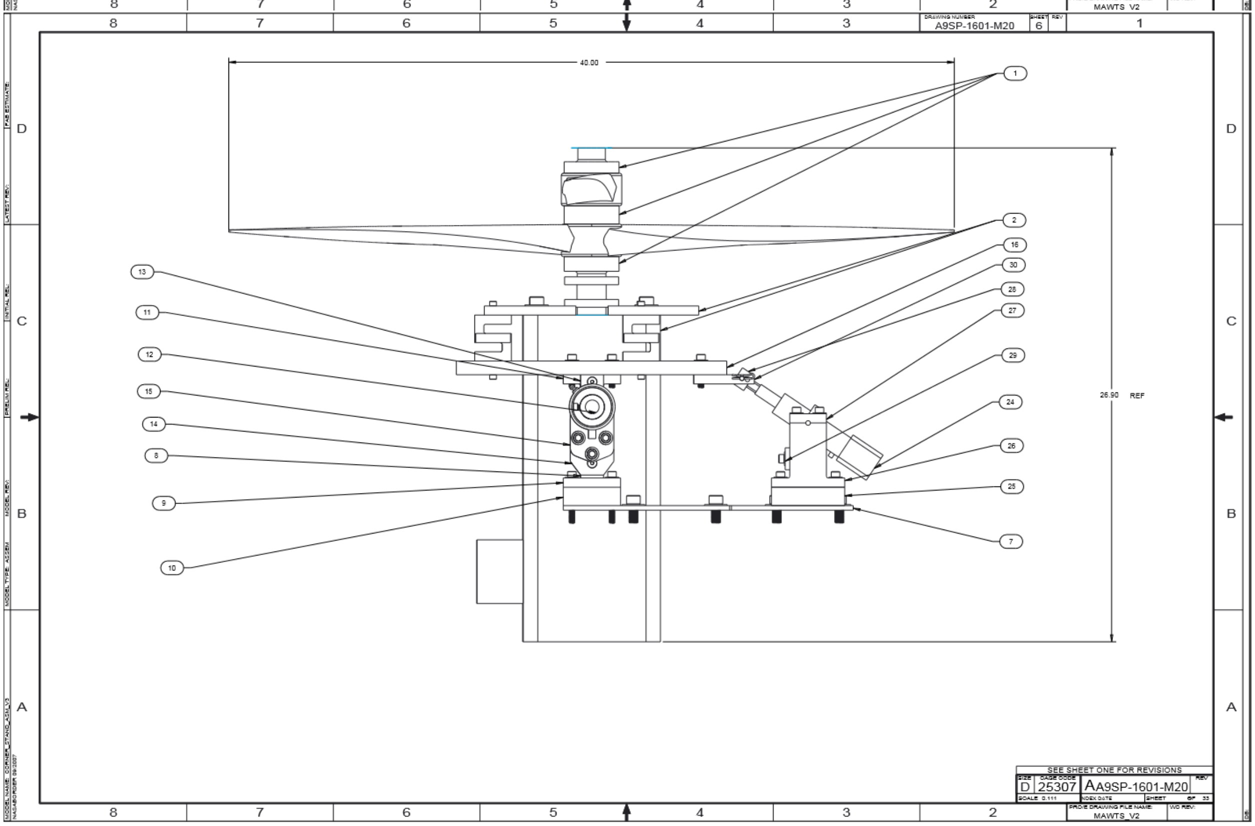
A9SP-1601-M20
40.00
26.90 REF
SEE SHEET ONE FOR REVISIONS
D 25307 AA9SP-1601-M20
MAWTS_V2

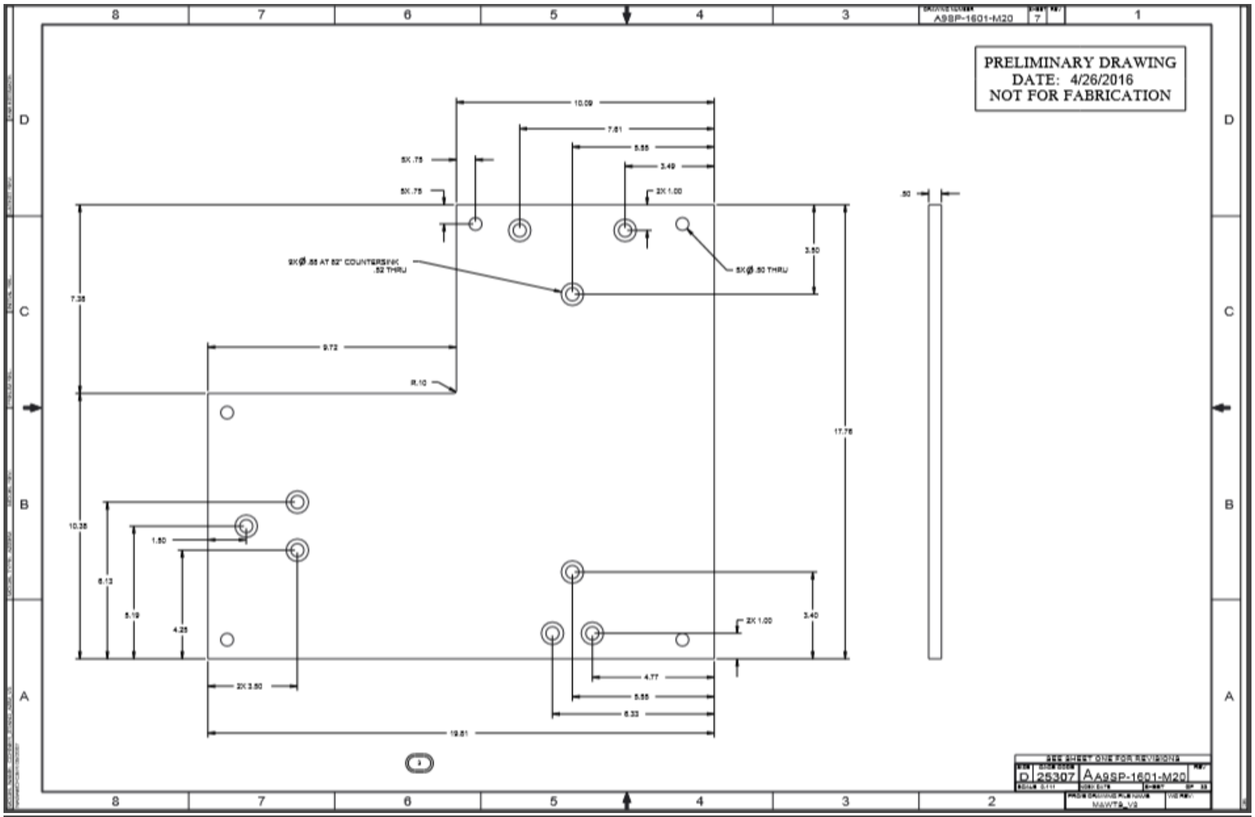
A9SP-1601-M20
PRELIMINARY DRAWING
DATE: 4/26/2016
NOT FOR FABRICATION
SEE SHEET ONE FOR REVISIONS
D 25307 AA9SP-1601-M20
MAWTR_V2

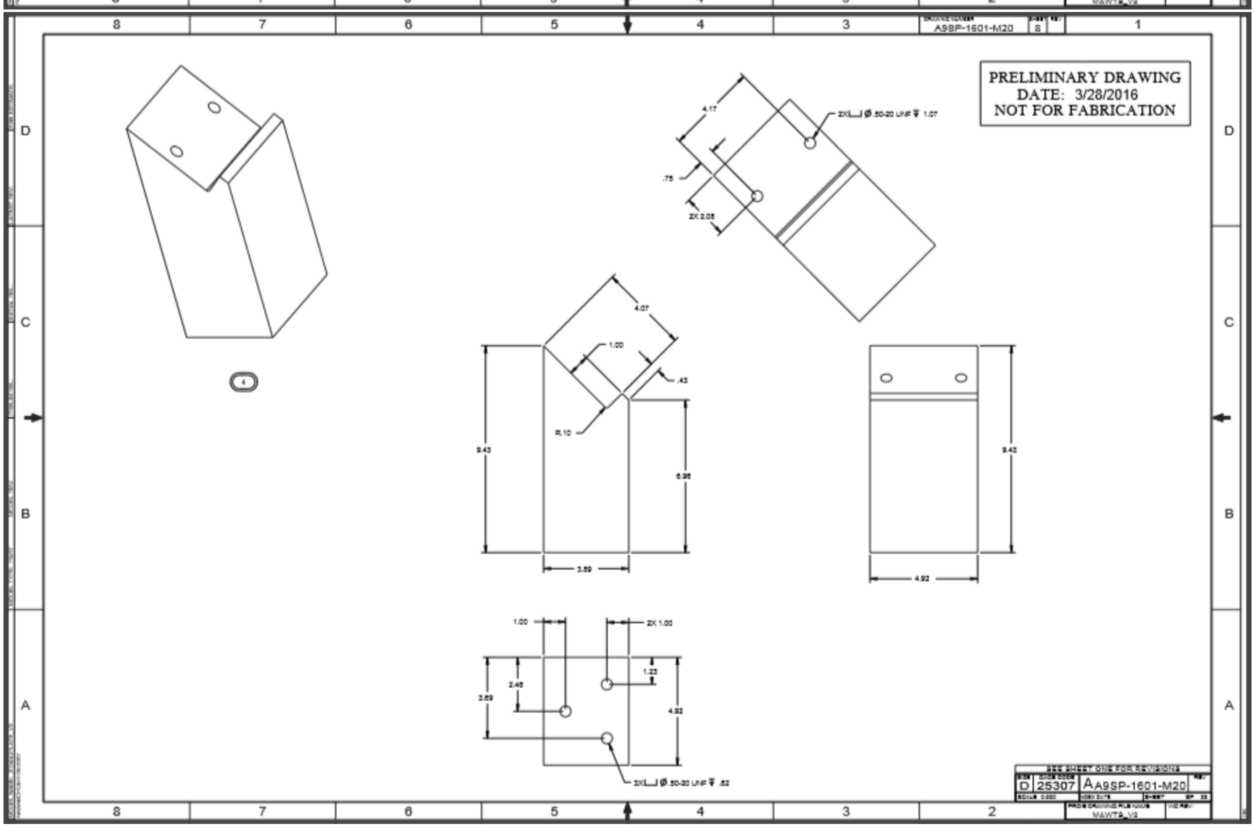
A9SP-1601-M20
PRELIMINARY DRAWING
DATE: 3/28/2016
NOT FOR FABRICATION
SEE SHEET ONE FOR REVISIONS
D 25307 AA9SP-1601-M20
MAWTR_V2

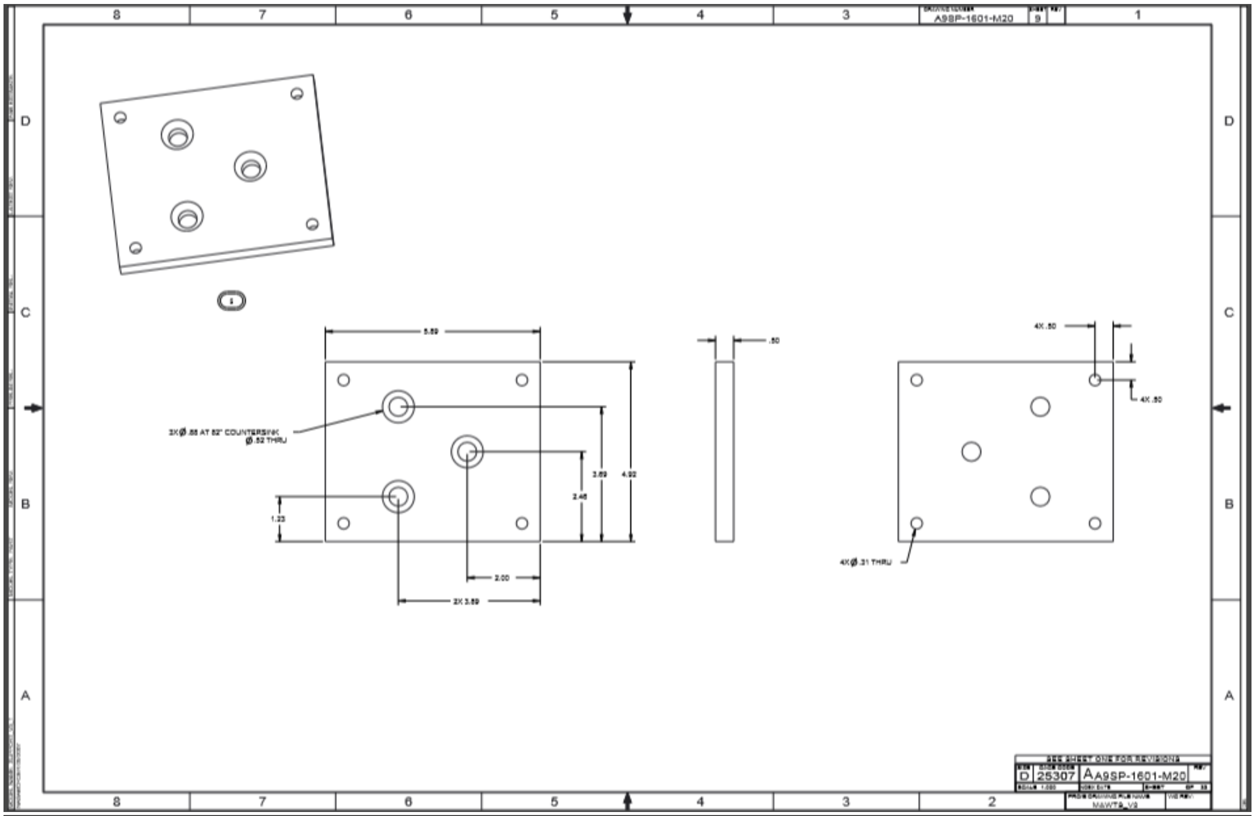
A9SP-1601-M20
9
5.89
.50
4X .50
4X .50
3XØ .88 AT 82° COUNTERSINK
Ø .52 THRU
3.69
4.92
2.46
1.23
2.00
2X 3.89
4XØ .31 THRU
SEE SHEET ONE FOR REVISIONS
D
25307
AA9SP-1601-M20
MAWTS_V2

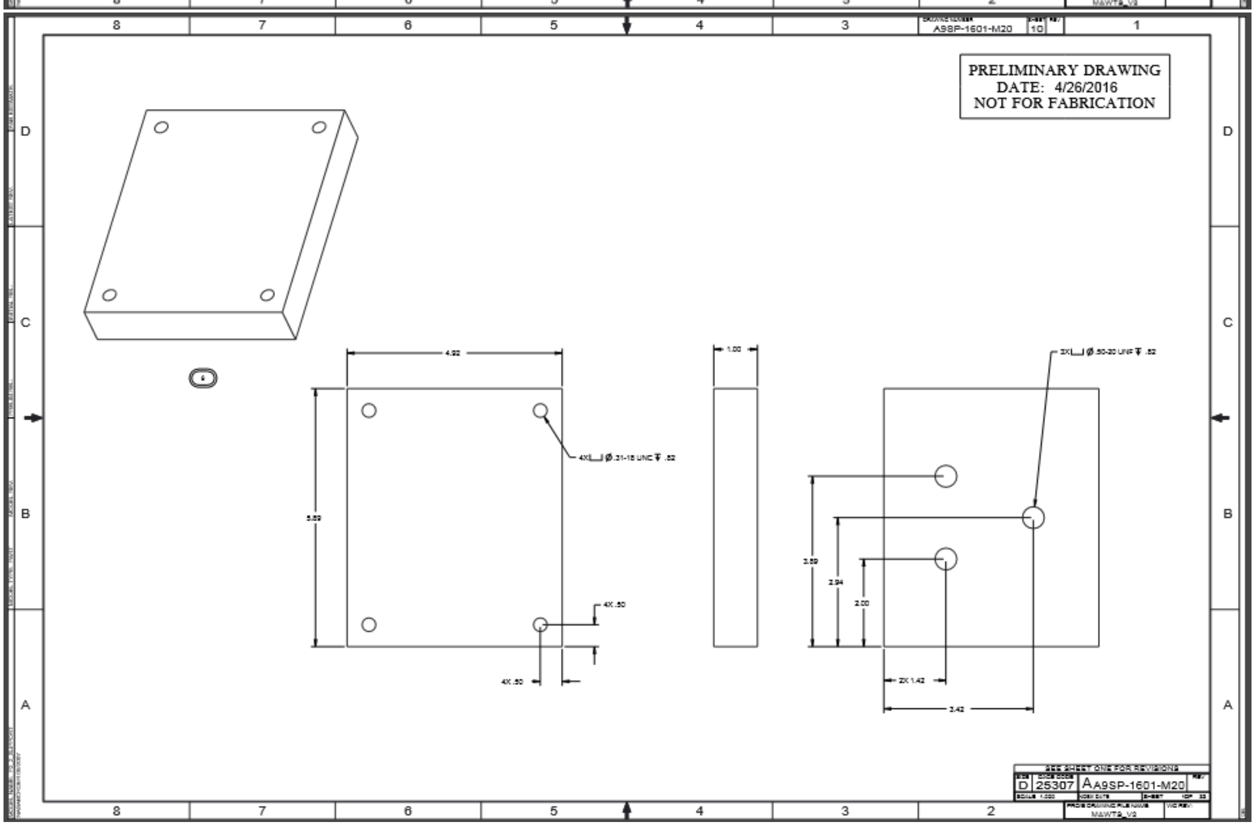
A9SP-1601-M20
10
PRELIMINARY DRAWING
DATE: 4/26/2016
NOT FOR FABRICATION
4.92
1.00
3X Ø .50-20 UNF ↧ .82
4X Ø .31-18 UNC ↧ .82
5.89
4X .50
4X .50
3.89
2.94
2.00
2X 1.42
3.42
SEE SHEET ONE FOR REVISIONS
D
25307
AA9SP-1601-M20
MAWTS_V2

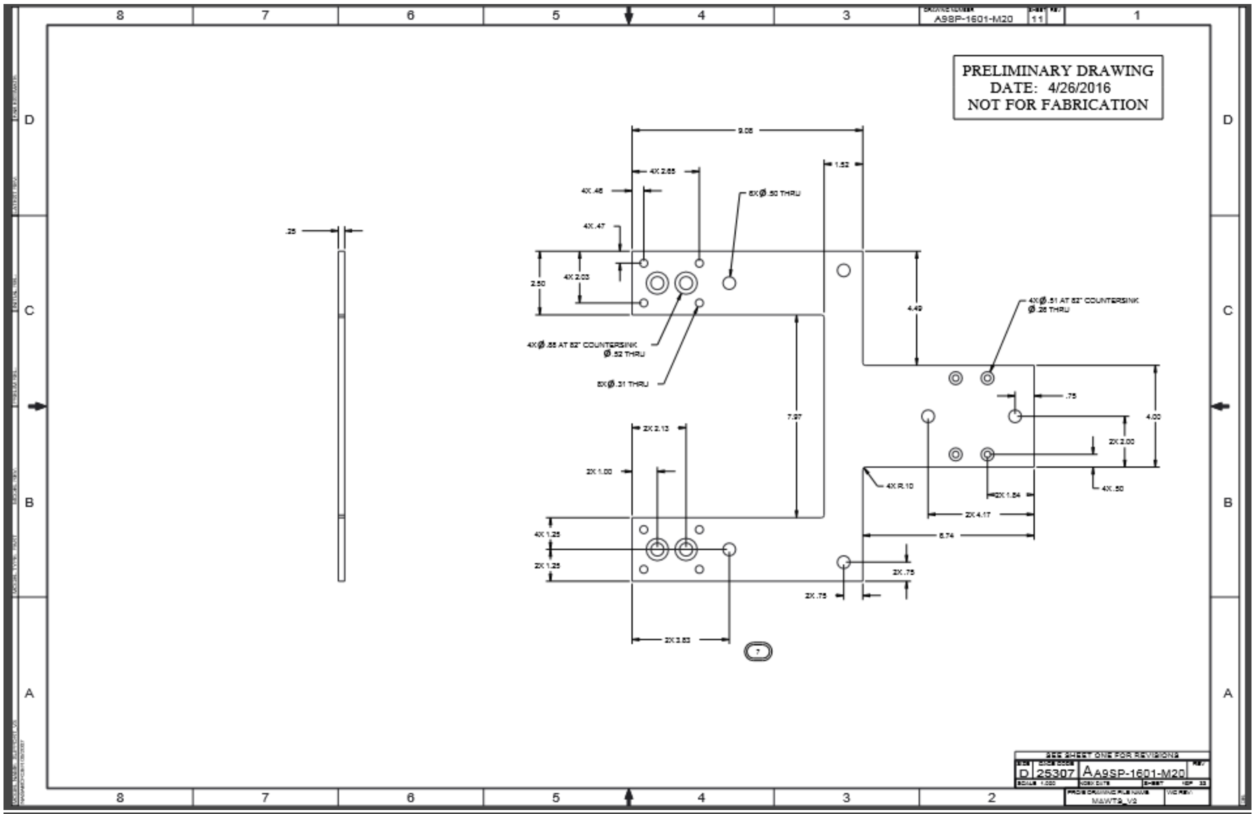
A9SP-1601-M20
11
PRELIMINARY DRAWING
DATE: 4/26/2016
NOT FOR FABRICATION
SEE SHEET ONE FOR REVISIONS
D 25307 A A9SP-1601-M20
MAWTP_V2

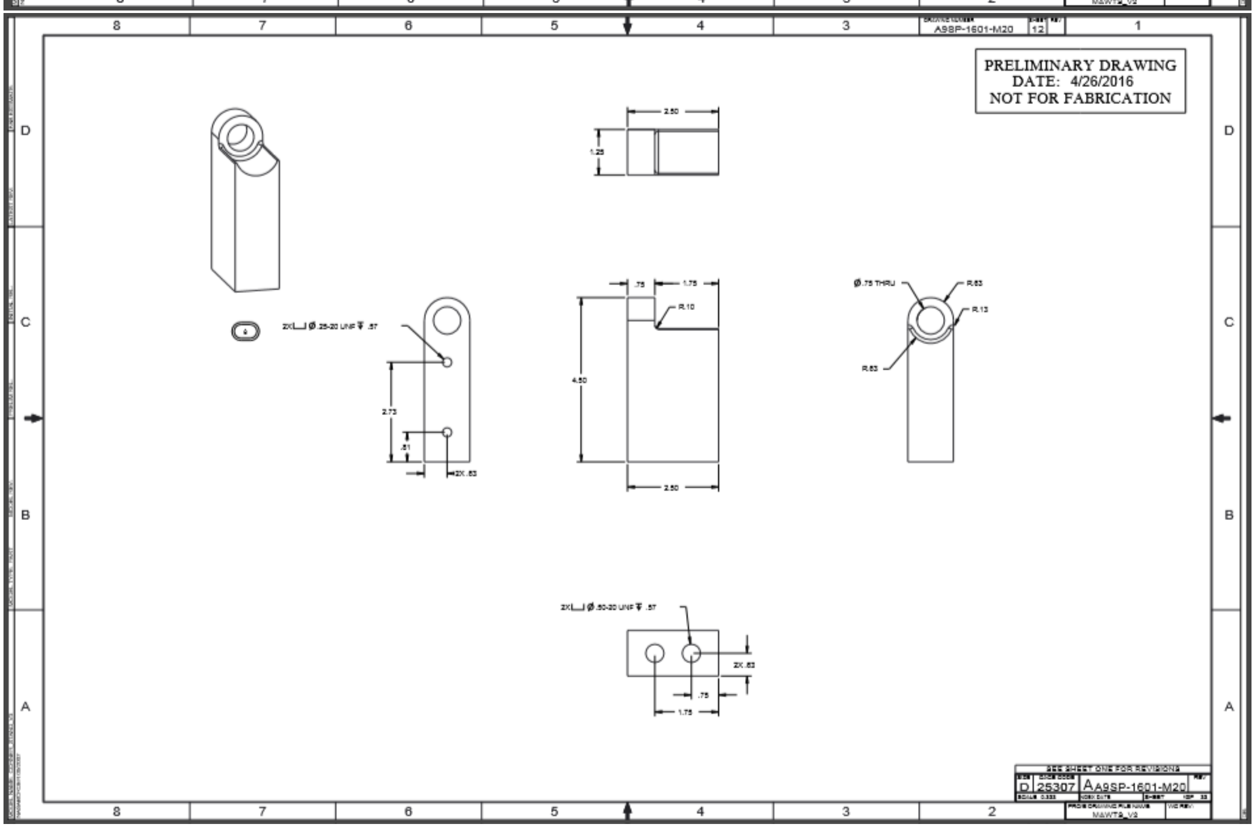
A9SP-1601-M20
12
PRELIMINARY DRAWING
DATE: 4/26/2016
NOT FOR FABRICATION
SEE SHEET ONE FOR REVISIONS
D 25307 A A9SP-1601-M20
MAWTP_V2

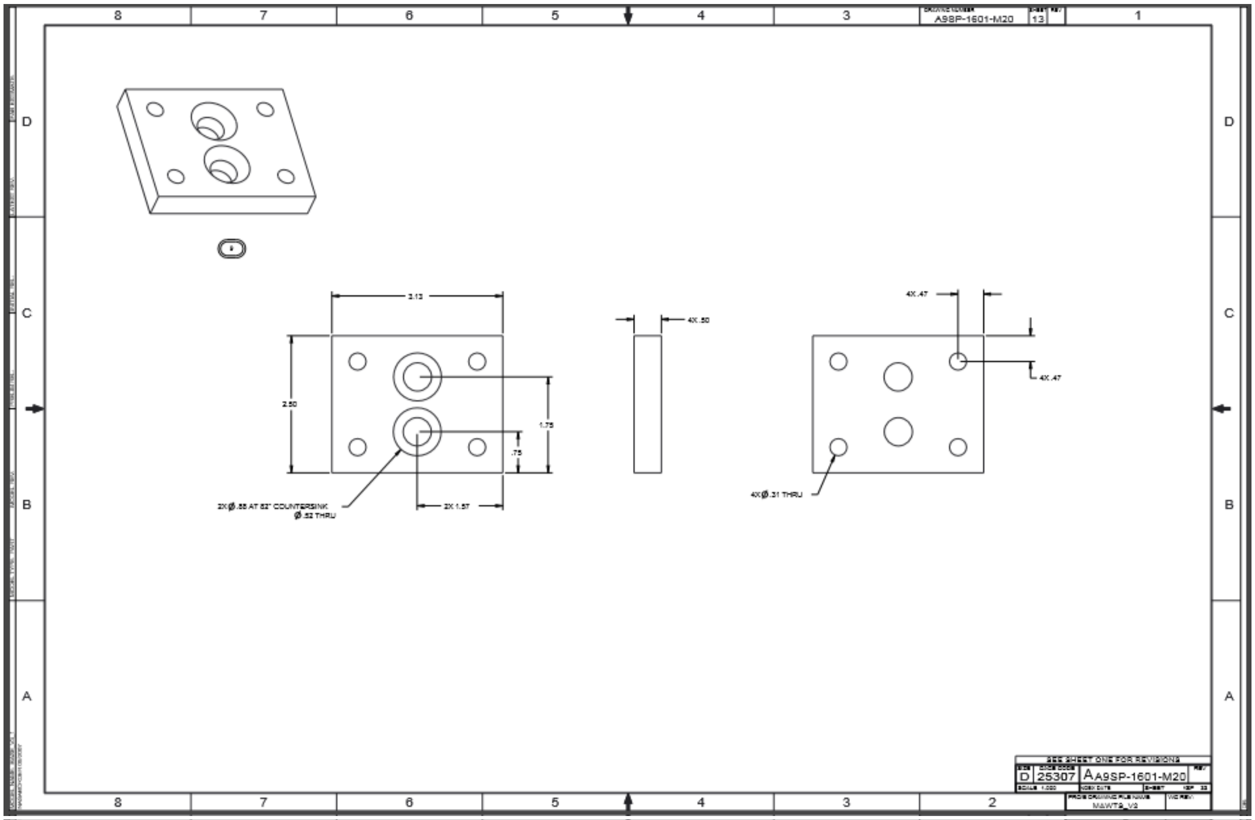
A9SP-1601-M20
13
3.13
4X .50
4X .47
2.50
1.75
.75
2X 1.57
4X Ø.31 THRU
SEE SHEET ONE FOR REVISIONS
D 25307 A9SP-1601-M20
MAWTR_V2

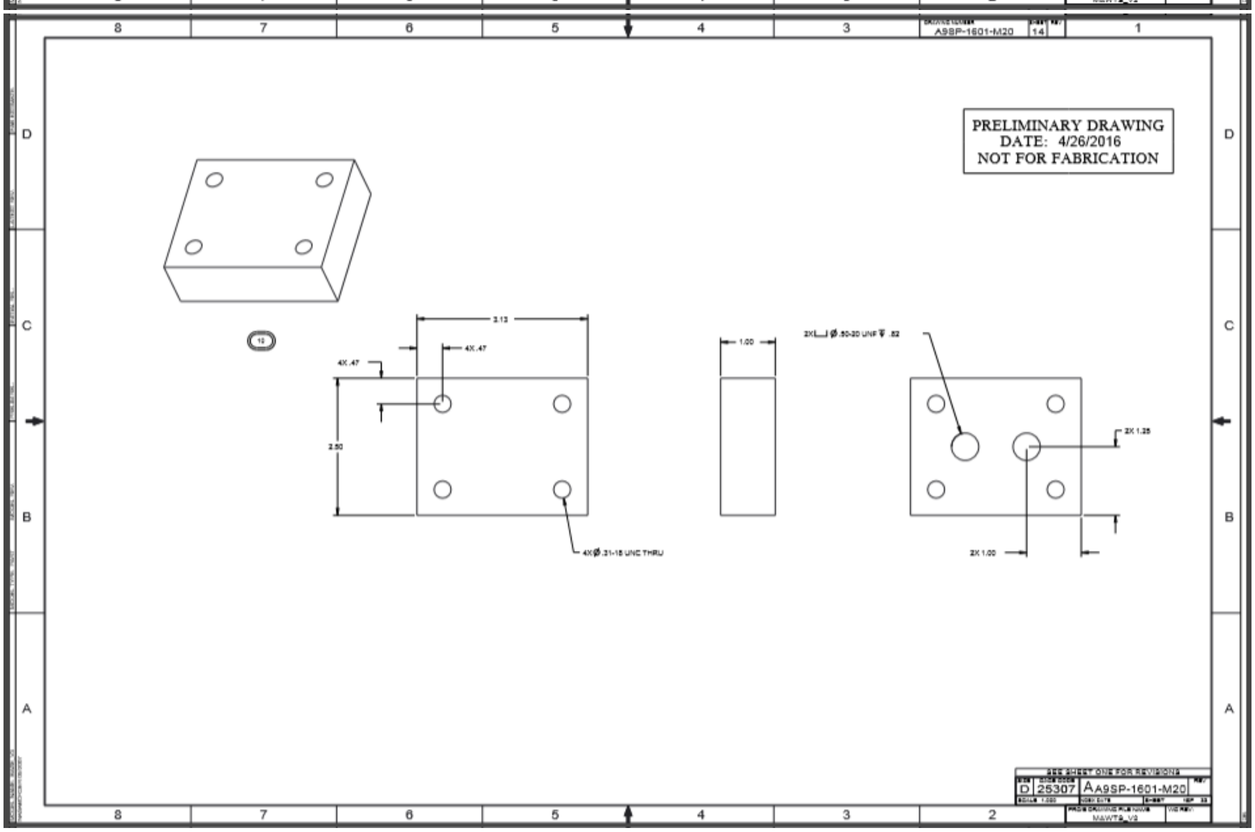
A9SP-1601-M20
14
PRELIMINARY DRAWING
DATE: 4/26/2016
NOT FOR FABRICATION
3.13
4X .47
1.00
2.50
4X Ø.31-18 UNC THRU
2X 1.25
2X 1.00
SEE SHEET ONE FOR REVISIONS
D 25307 A9SP-1601-M20
MAWTR_V2

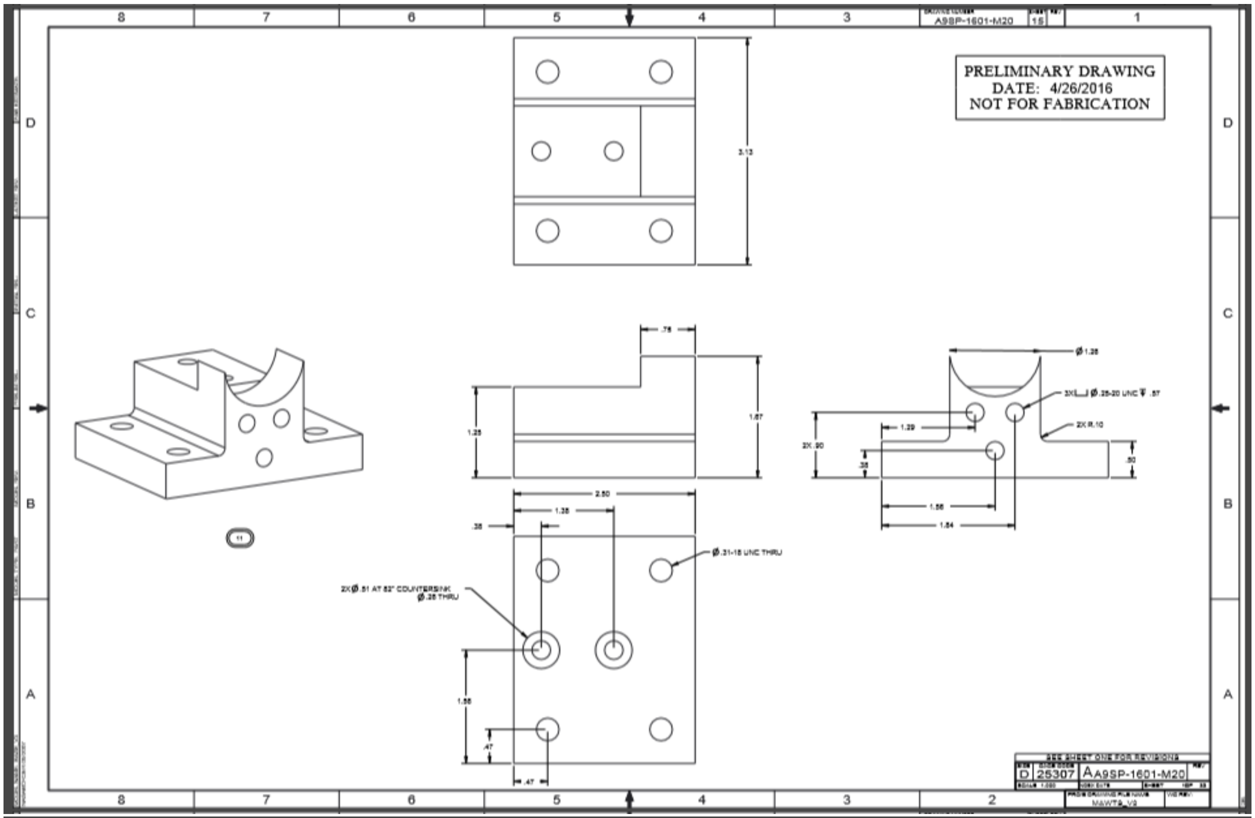
A9SP-1601-M20
PRELIMINARY DRAWING
DATE: 4/26/2016
NOT FOR FABRICATION
25307
A9SP-1601-M20

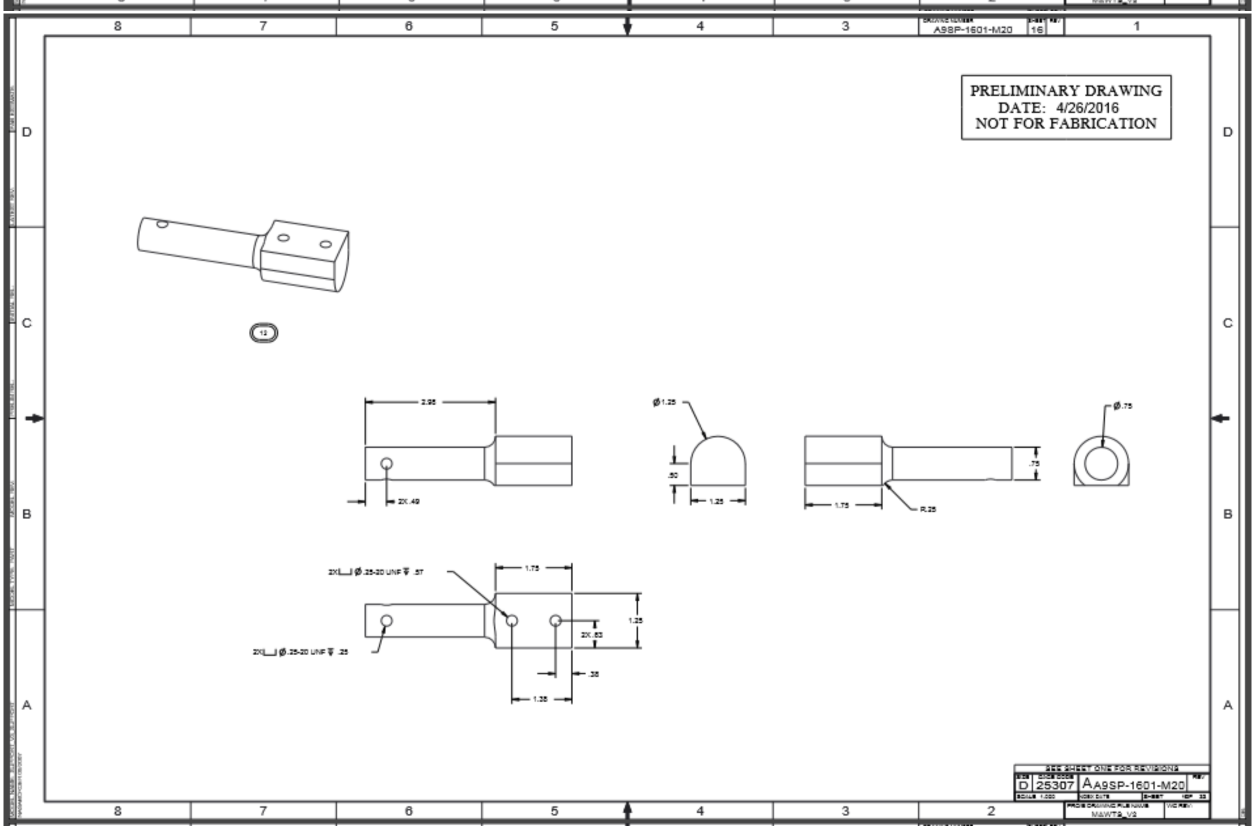
A9SP-1601-M20
PRELIMINARY DRAWING
DATE: 4/26/2016
NOT FOR FABRICATION
25307
A9SP-1601-M20

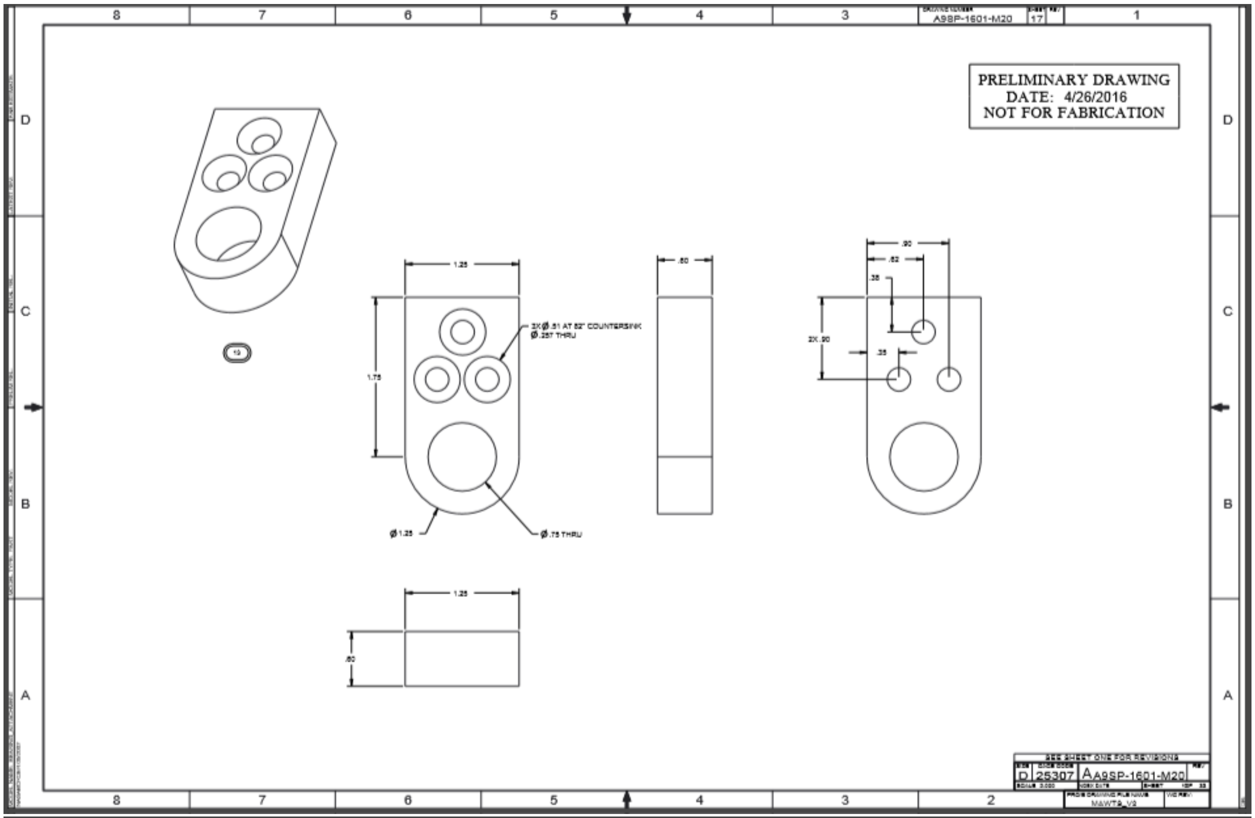
A9SP-1601-M20
17
PRELIMINARY DRAWING
DATE: 4/26/2016
NOT FOR FABRICATION
1.25
.50
.90
.62
3X Ø.51 AT 82° COUNTERSINK
Ø.257 THRU
1.75
2X .90
.35
Ø1.25
Ø.75 THRU
D 25307 A9SP-1601-M20
MAWTA_V2

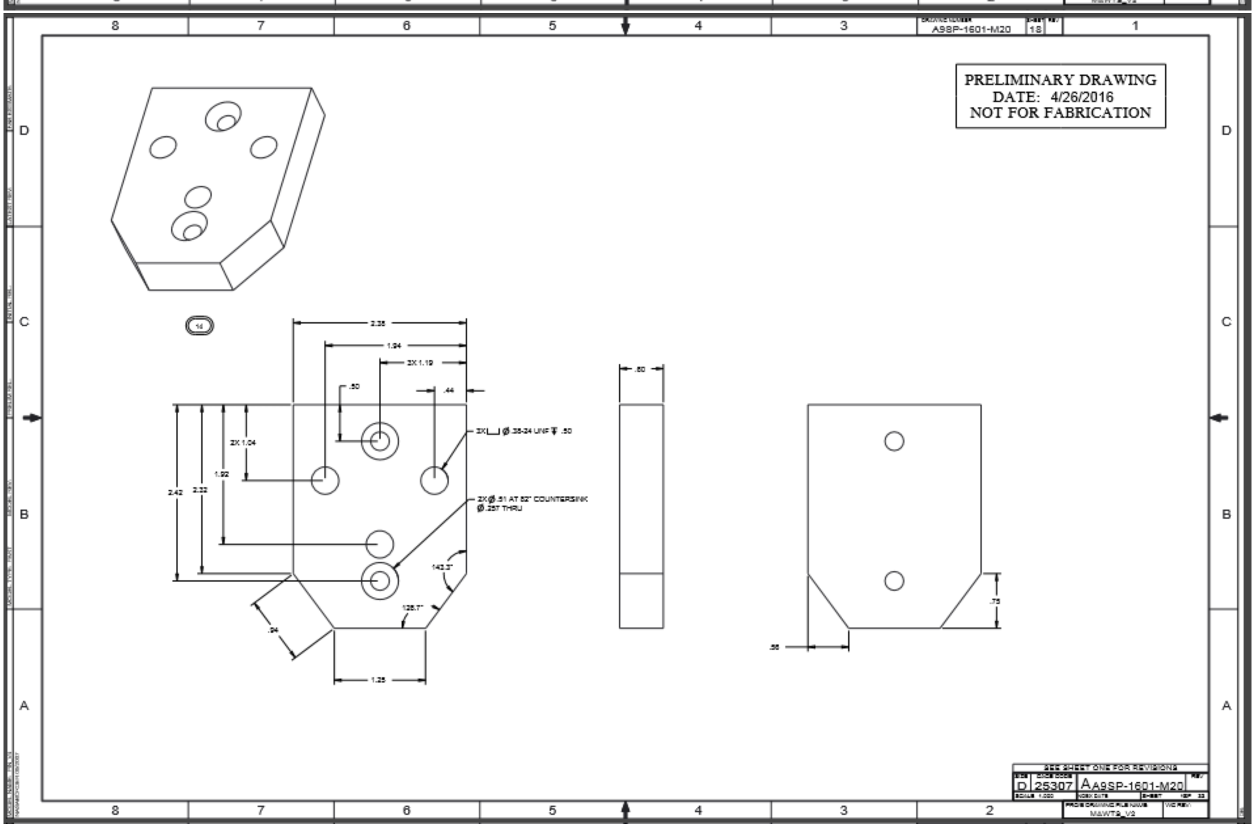
A9SP-1601-M20
18
PRELIMINARY DRAWING
DATE: 4/26/2016
NOT FOR FABRICATION
2.35
1.94
2X 1.19
.50
.44
2X 1.04
1.92
2.42
2.32
2X Ø.51 AT 82° COUNTERSINK
Ø.257 THRU
143.3°
125.7°
.94
1.25
.50
.75
.56
D 25307 A9SP-1601-M20
MAWTA_V2

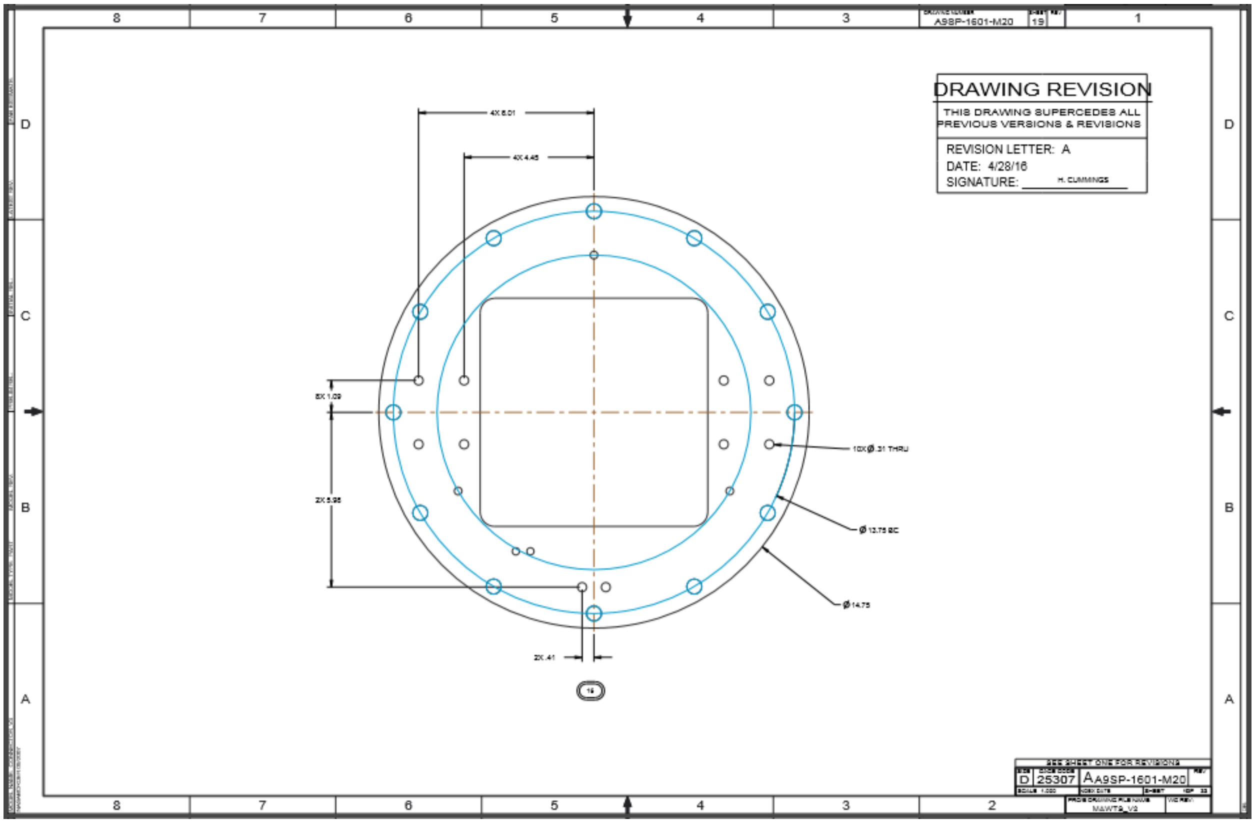

DRAWING REVISION
THIS DRAWING SUPERCEDES ALL PREVIOUS VERSIONS & REVISIONS
REVISION LETTER: A
DATE: 4/28/16
SIGNATURE:
A9SP-1601-M20
19
4X 6.01
4X 4.45
10X Ø.31 THRU
Ø13.75 BC
Ø14.75
2X 5.95
2X .41
D 25307 A A9SP-1601-M20

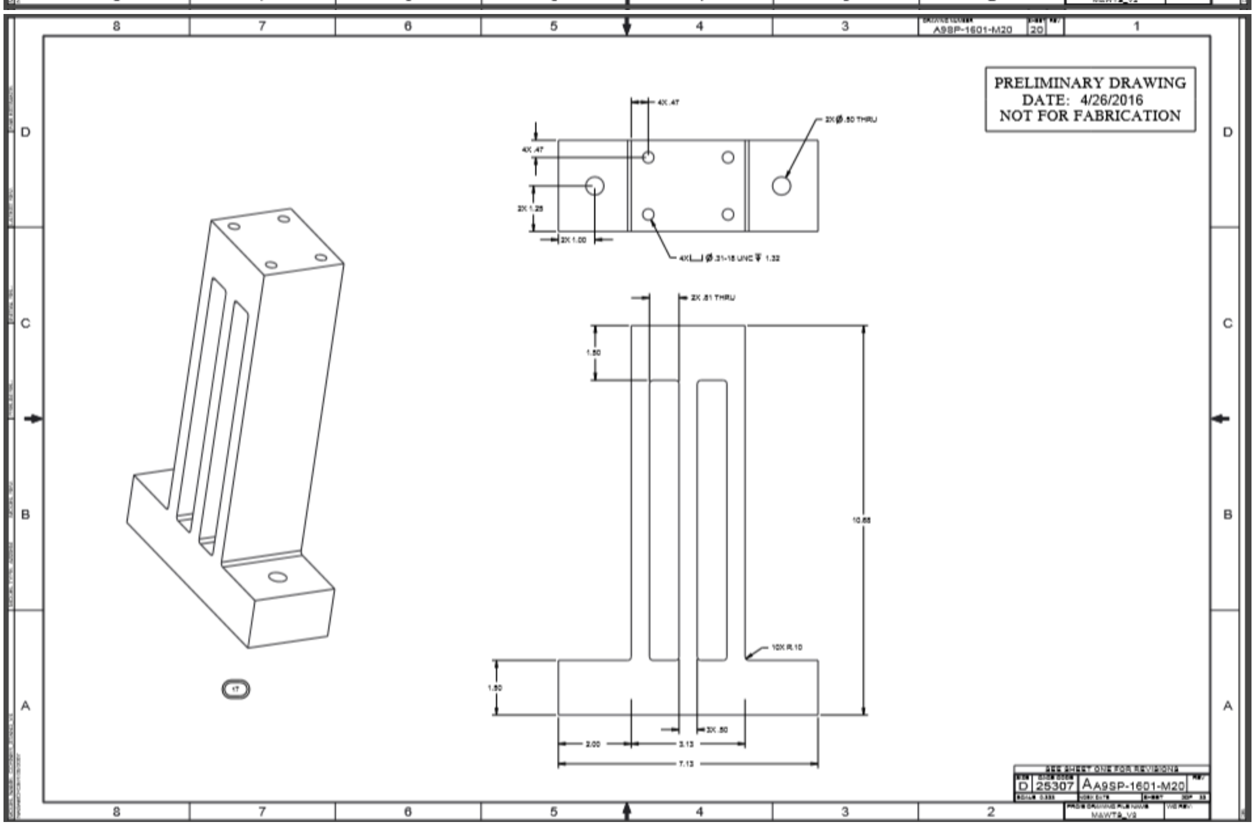

PRELIMINARY DRAWING
DATE: 4/26/2016
NOT FOR FABRICATION
A9SP-1601-M20
20
4X .47
2X Ø.50 THRU
2X 1.25
2X 1.00
2X .81 THRU
1.50
10.68
10X R.10
2.00
3.13
3X .50
7.13
D 25307 A A9SP-1601-M20

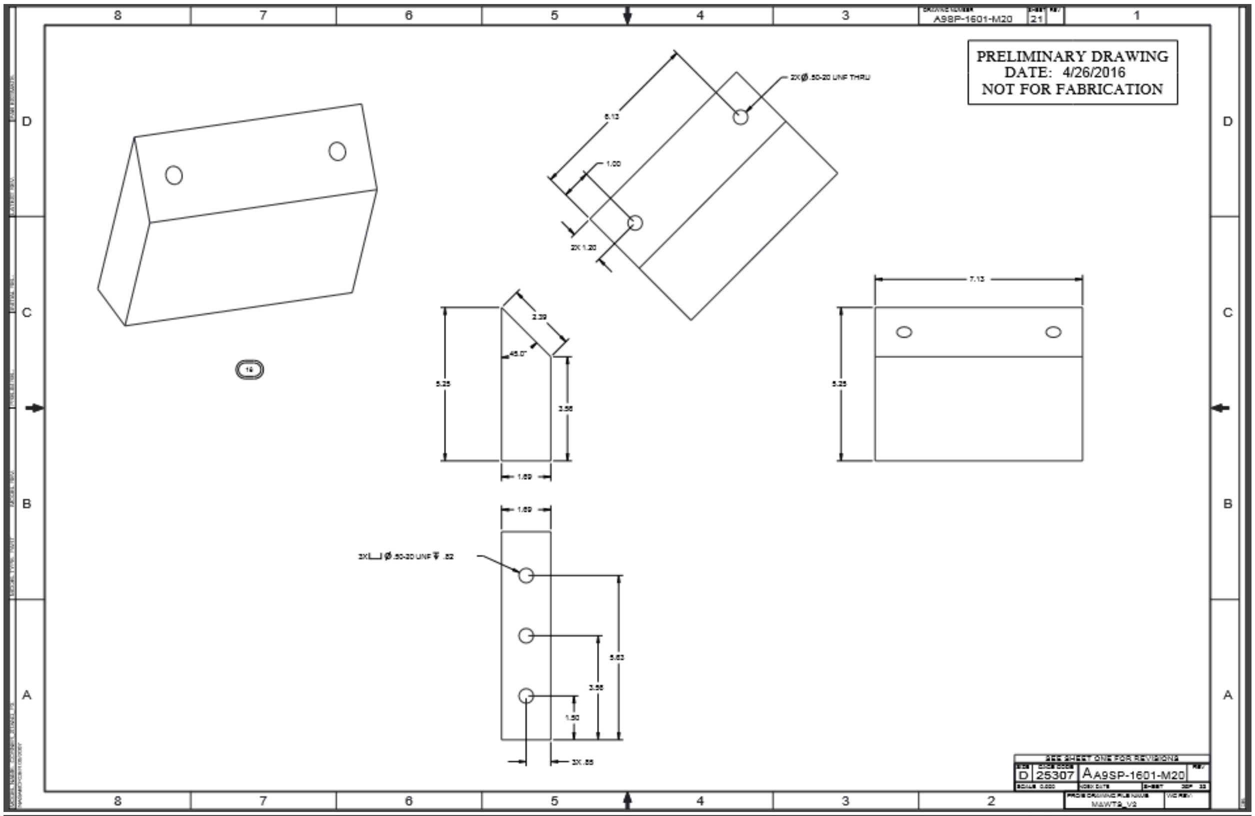
PRELIMINARY DRAWING
DATE: 4/26/2016
NOT FOR FABRICATION
A9SP-1601-M20
21
2X Ø.50-20 UNF THRU
6.13
1.00
2X 1.20
2.39
45.0°
5.25
3.56
1.69
7.13
5.25
1.69
3X Ø.50-20 UNF .82
5.63
3.56
1.50
3X .85
SEE SHEET ONE FOR REVISIONS
D
25307
A9SP-1601-M20
MAWTP_V2

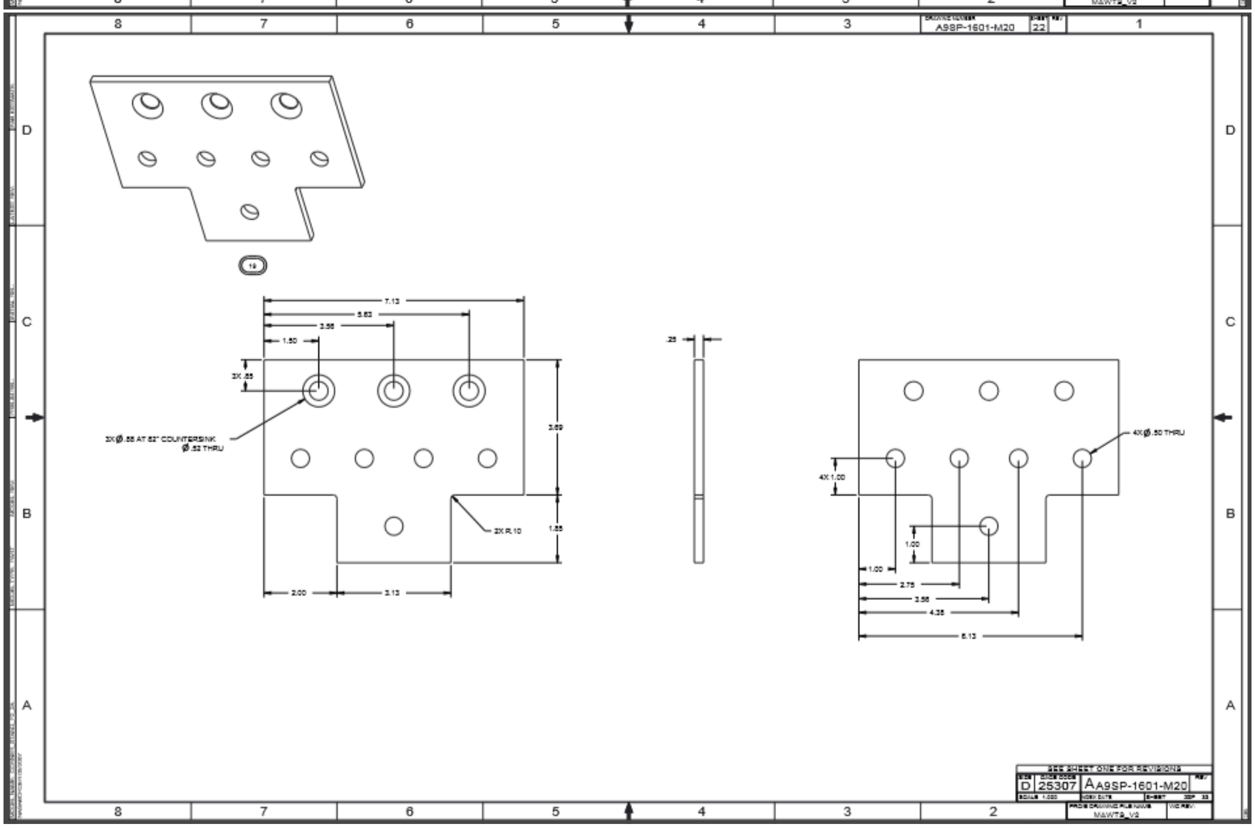
A9SP-1601-M20
22
7.13
5.63
3.56
1.50
3X .85
3X Ø.88 AT 82° COUNTERSINK
Ø.52 THRU
3.69
2X R.10
1.85
2.00
3.13
.25
4X Ø.50 THRU
4X 1.00
1.00
1.00
2.75
3.56
4.38
6.13
SEE SHEET ONE FOR REVISIONS
D
25307
A9SP-1601-M20
MAWTP_V2

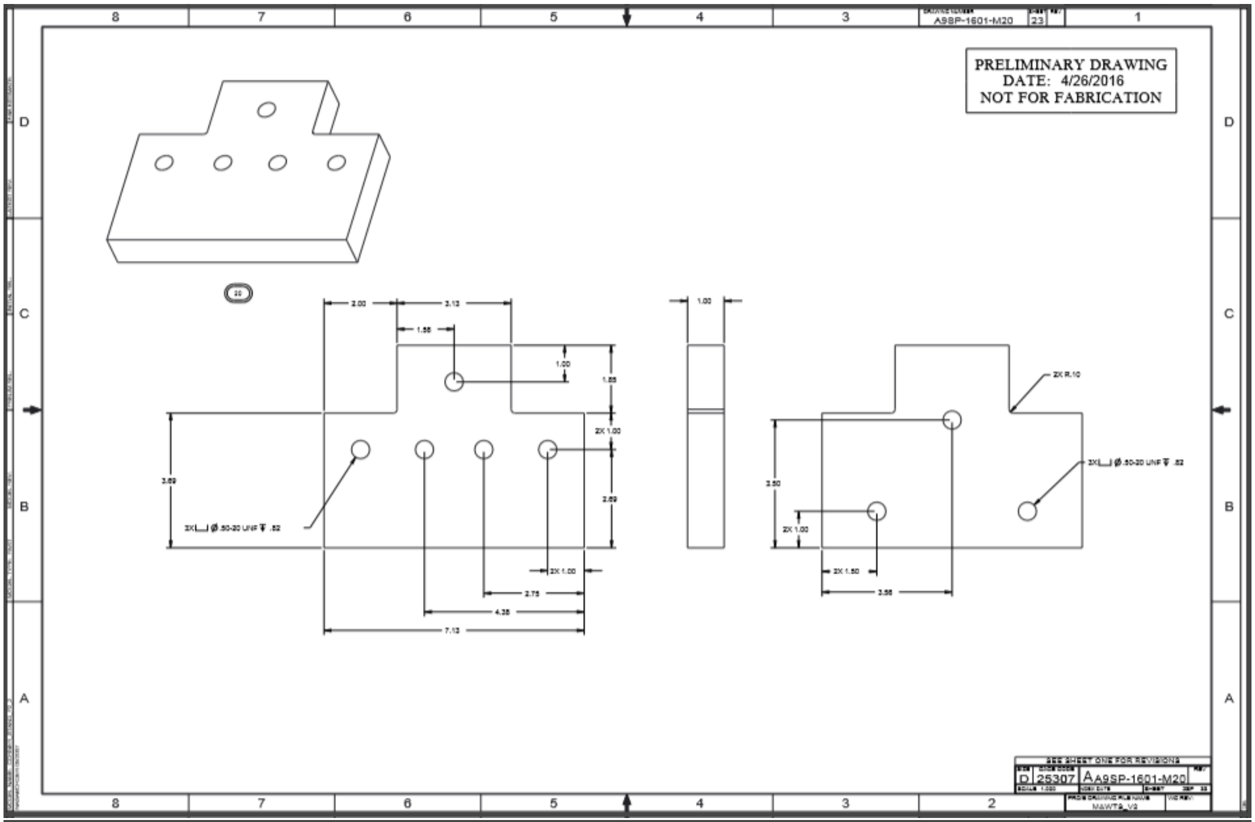
A9SP-1601-M20
23
PRELIMINARY DRAWING
DATE: 4/26/2016
NOT FOR FABRICATION
3X ⌴ Ø.50-20 UNF ↧ .62
2X R.10
SEE SHEET ONE FOR REVISIONS
D 25307 A9SP-1601-M20
MAWTS_V2

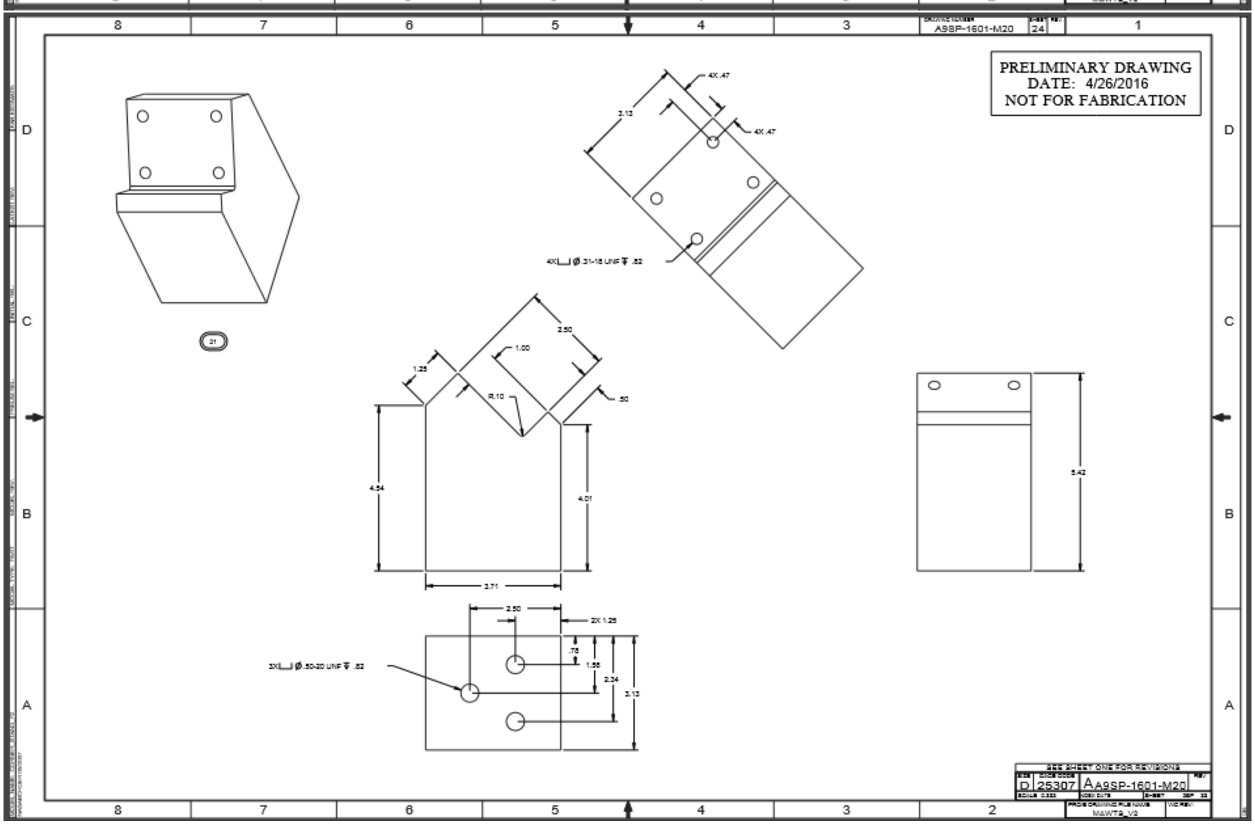
A9SP-1601-M20
24
PRELIMINARY DRAWING
DATE: 4/26/2016
NOT FOR FABRICATION
4X ⌴ Ø.31-18 UNF ↧ .62
3X ⌴ Ø.50-20 UNF ↧ .62
SEE SHEET ONE FOR REVISIONS
D 25307 A9SP-1601-M20
MAWTS_V2

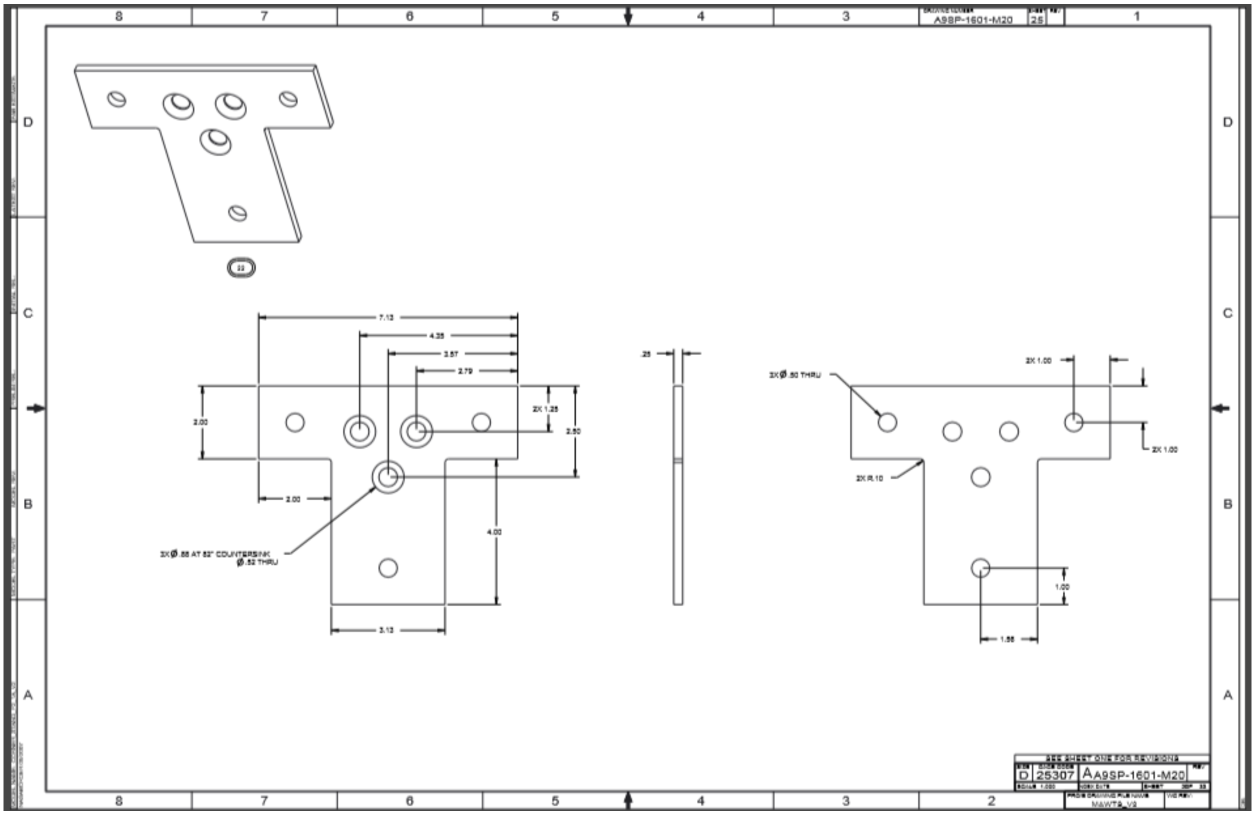
A9SP-1601-M20
25
D 25307
A9SP-1601-M20
MAWTP_V2

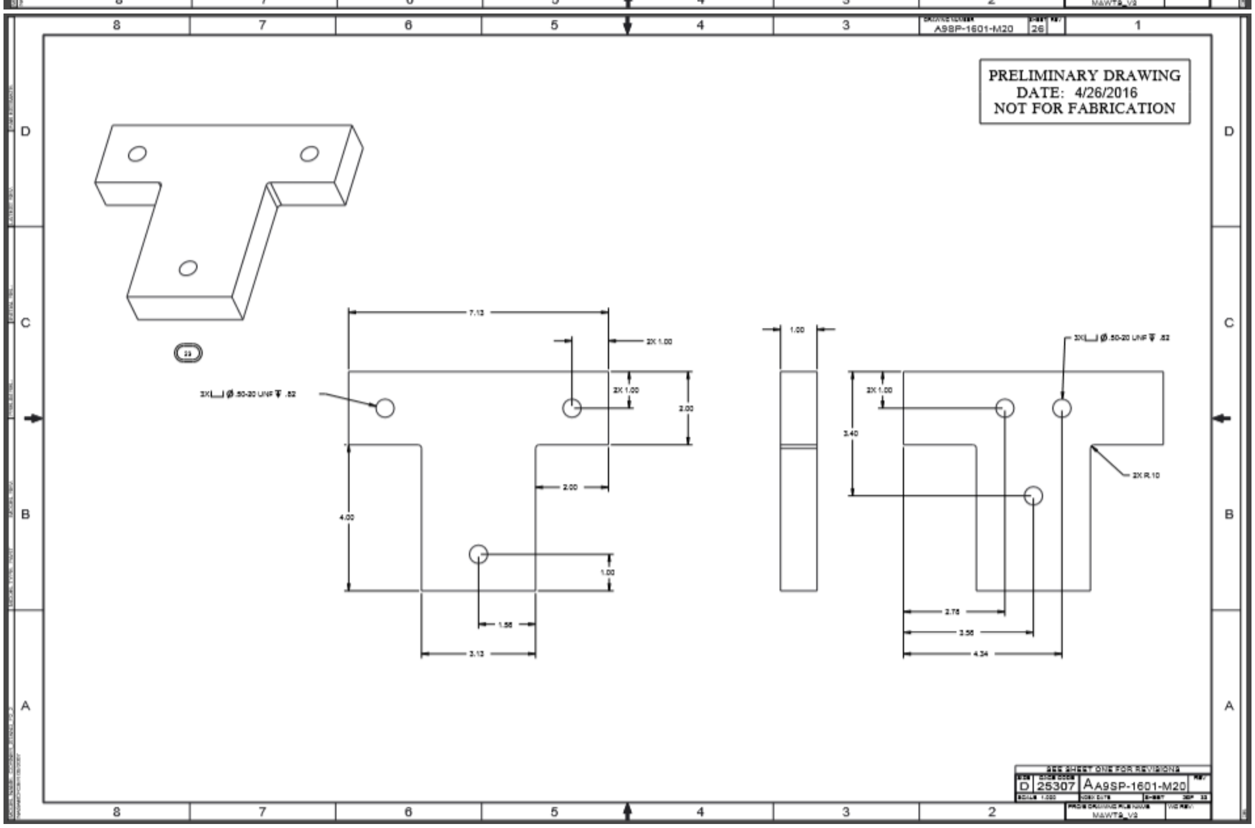
A9SP-1601-M20
26
PRELIMINARY DRAWING
DATE: 4/26/2016
NOT FOR FABRICATION
D 25307
A9SP-1601-M20
MAWTP_V2

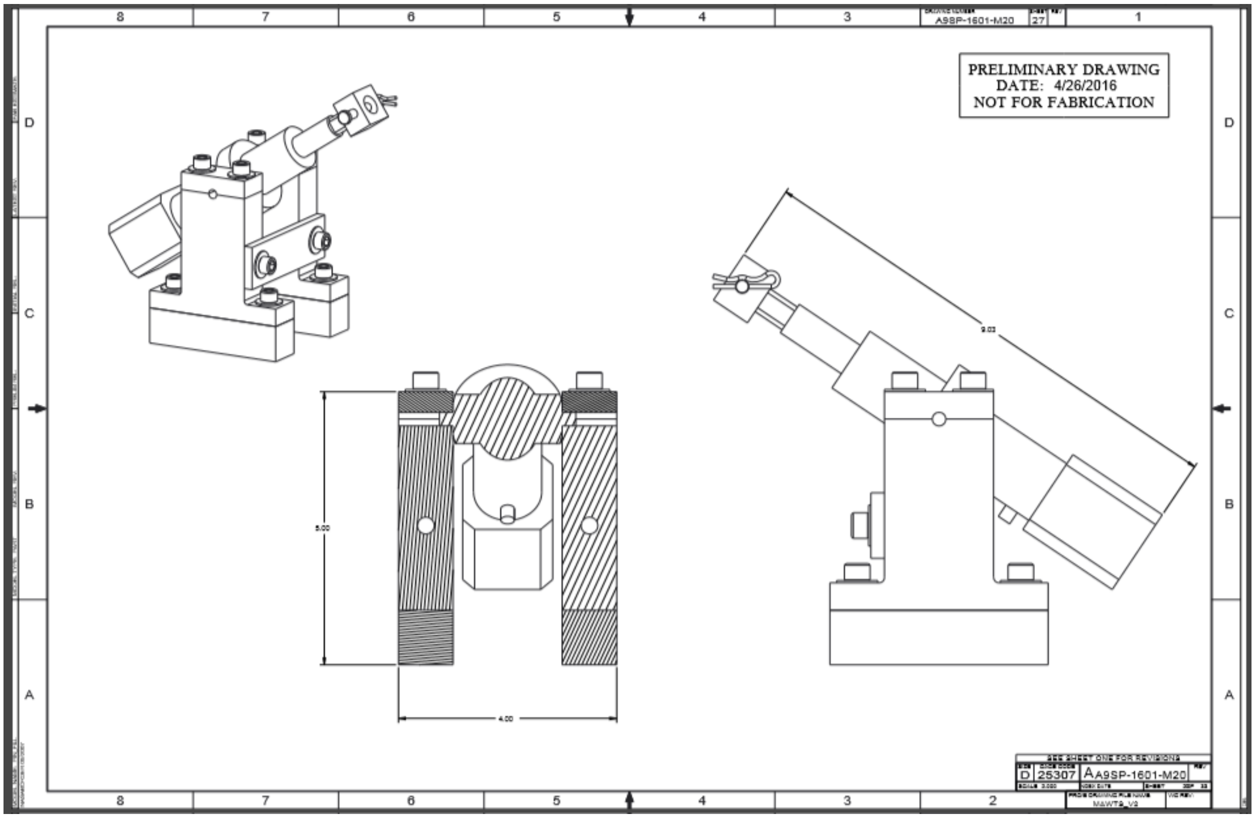
A9SP-1601-M20
27
PRELIMINARY DRAWING
DATE: 4/26/2016
NOT FOR FABRICATION
9.03
5.00
4.00
D 25307 A9SP-1601-M20
MAWTS_V2

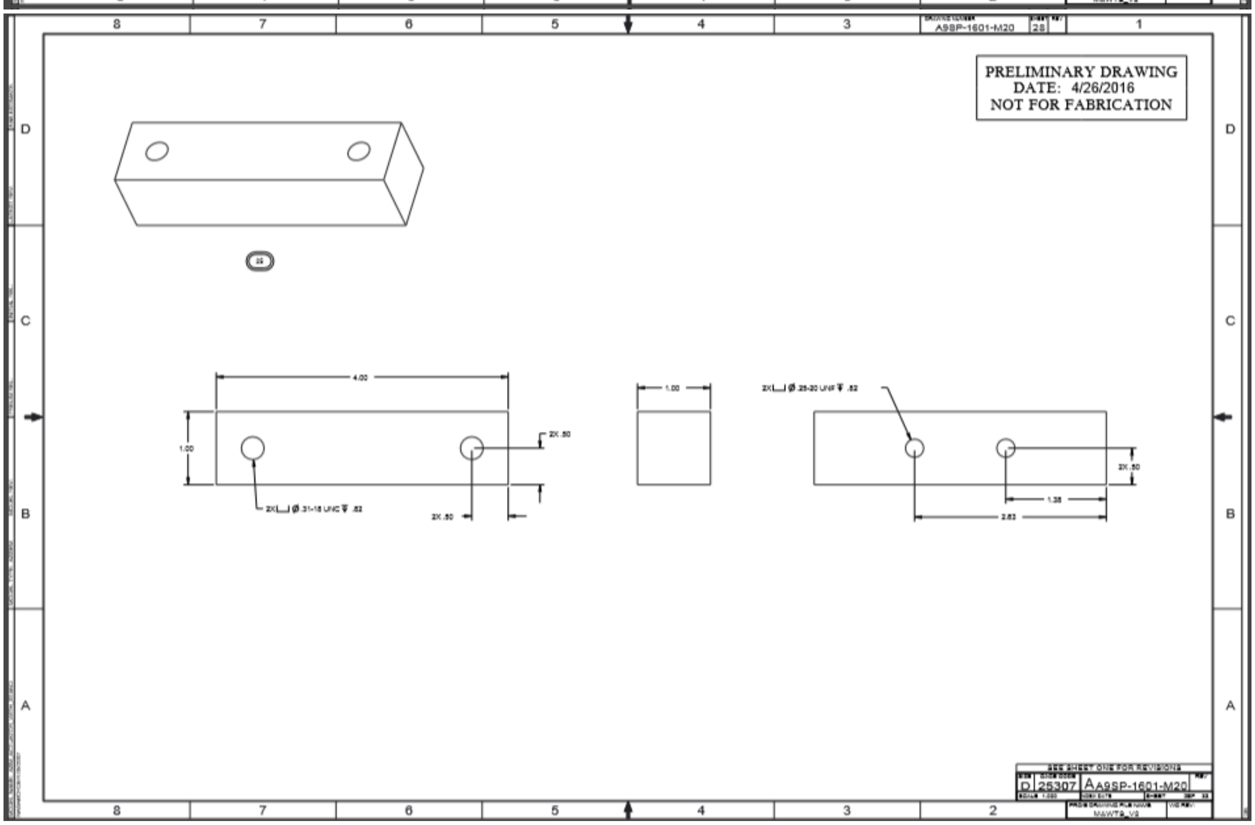
A9SP-1601-M20
28
PRELIMINARY DRAWING
DATE: 4/26/2016
NOT FOR FABRICATION
4.00
1.00
2X .50
2X .50
1.00
1.38
2.63
D 25307 A9SP-1601-M20
MAWTS_V2

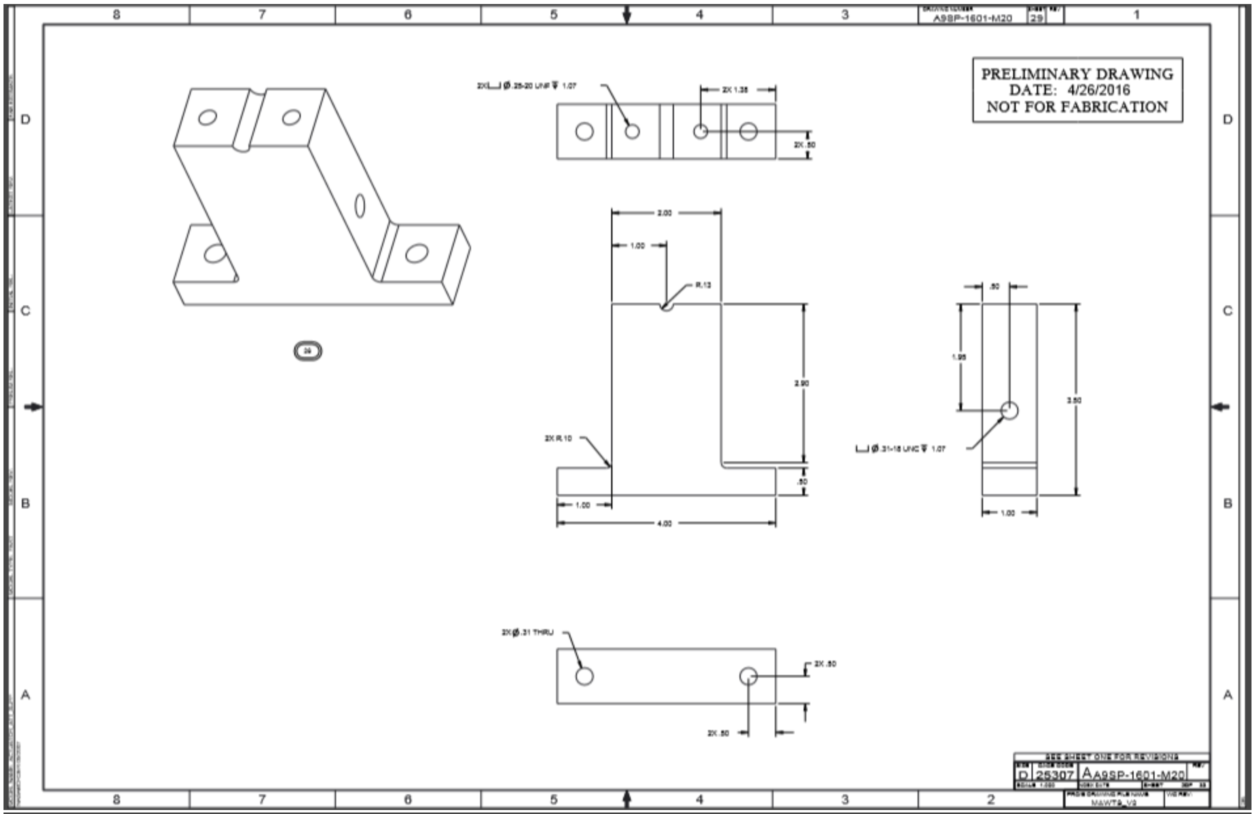
PRELIMINARY DRAWING
DATE: 4/26/2016
NOT FOR FABRICATION
A9SP-1601-M20
D 25307 A9SP-1601-M20

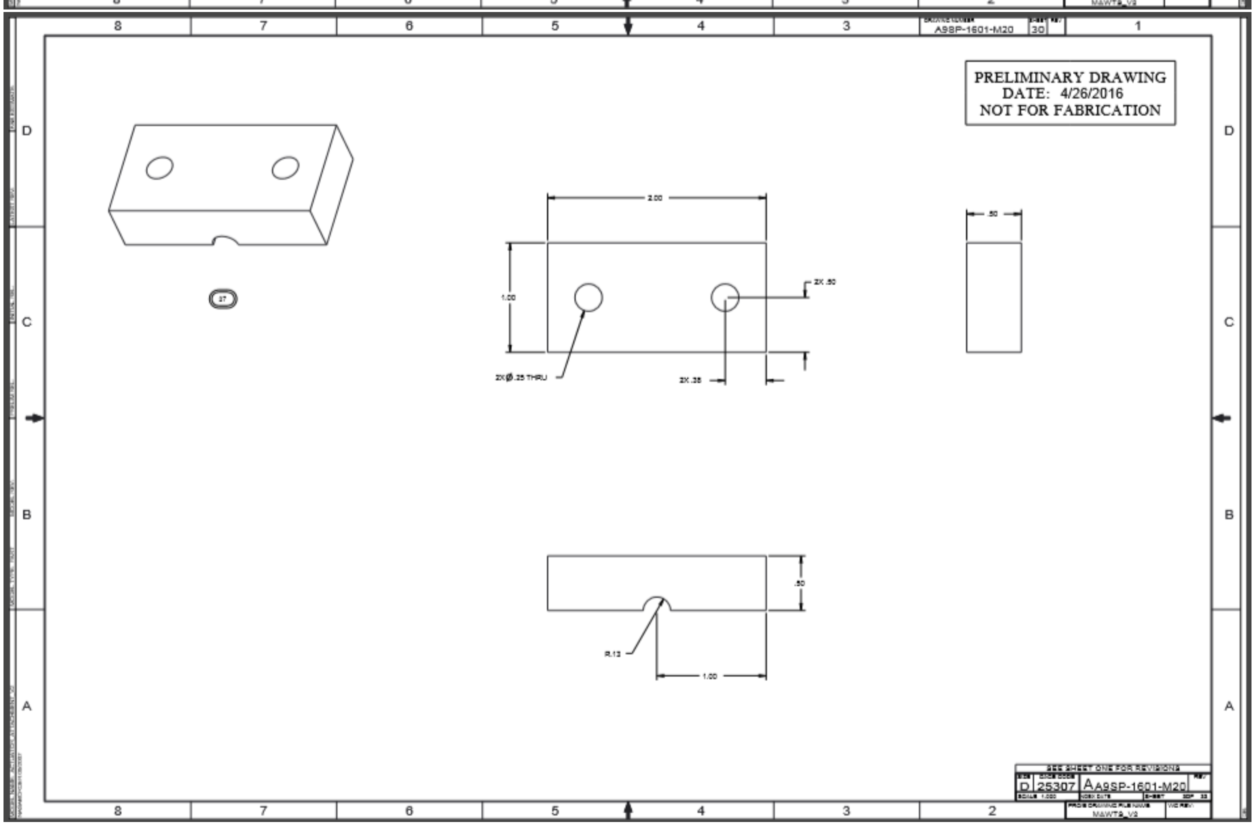
PRELIMINARY DRAWING
DATE: 4/26/2016
NOT FOR FABRICATION
A9SP-1601-M20
D 25307 A9SP-1601-M20

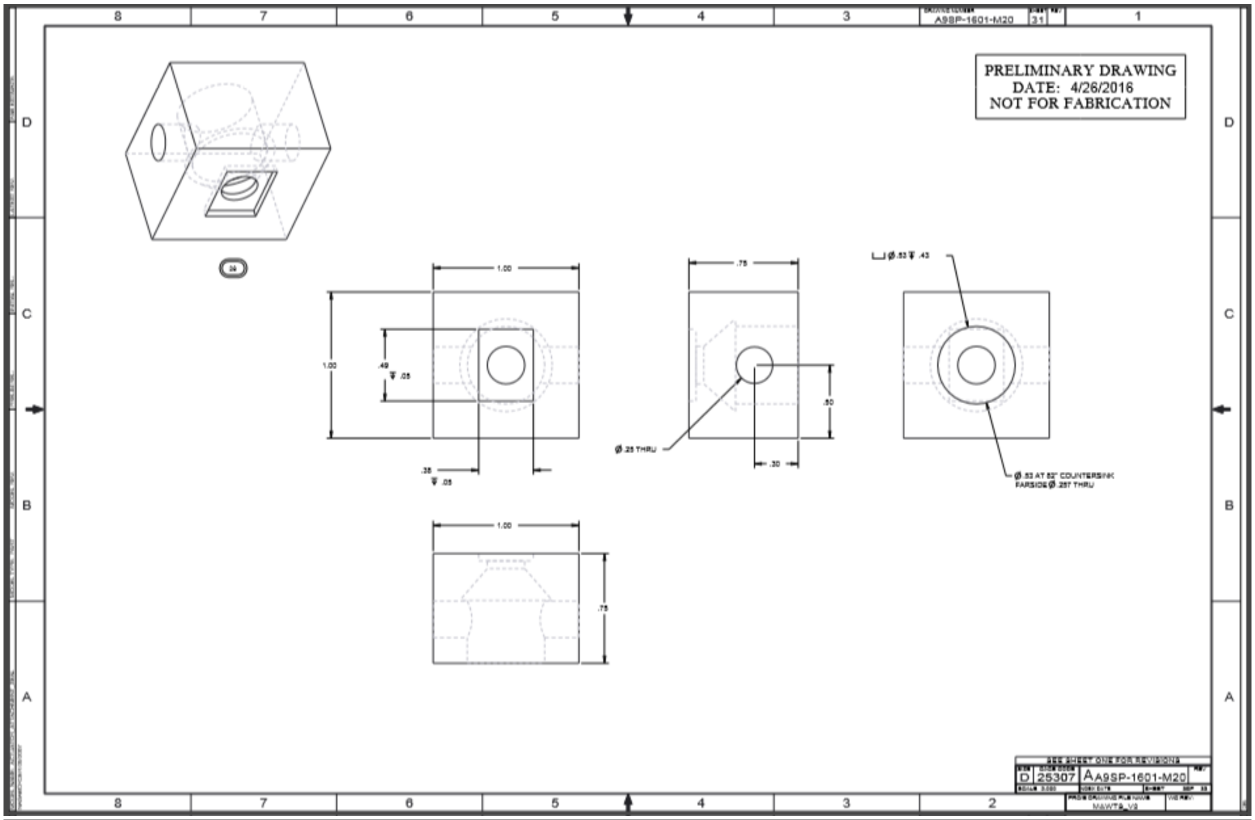
A9SP-1601-M20
31
PRELIMINARY DRAWING
DATE: 4/26/2016
NOT FOR FABRICATION
1.00
.75
1.00
Ø.25 THRU
.30
.50
.75
D 25307 AA9SP-1601-M20

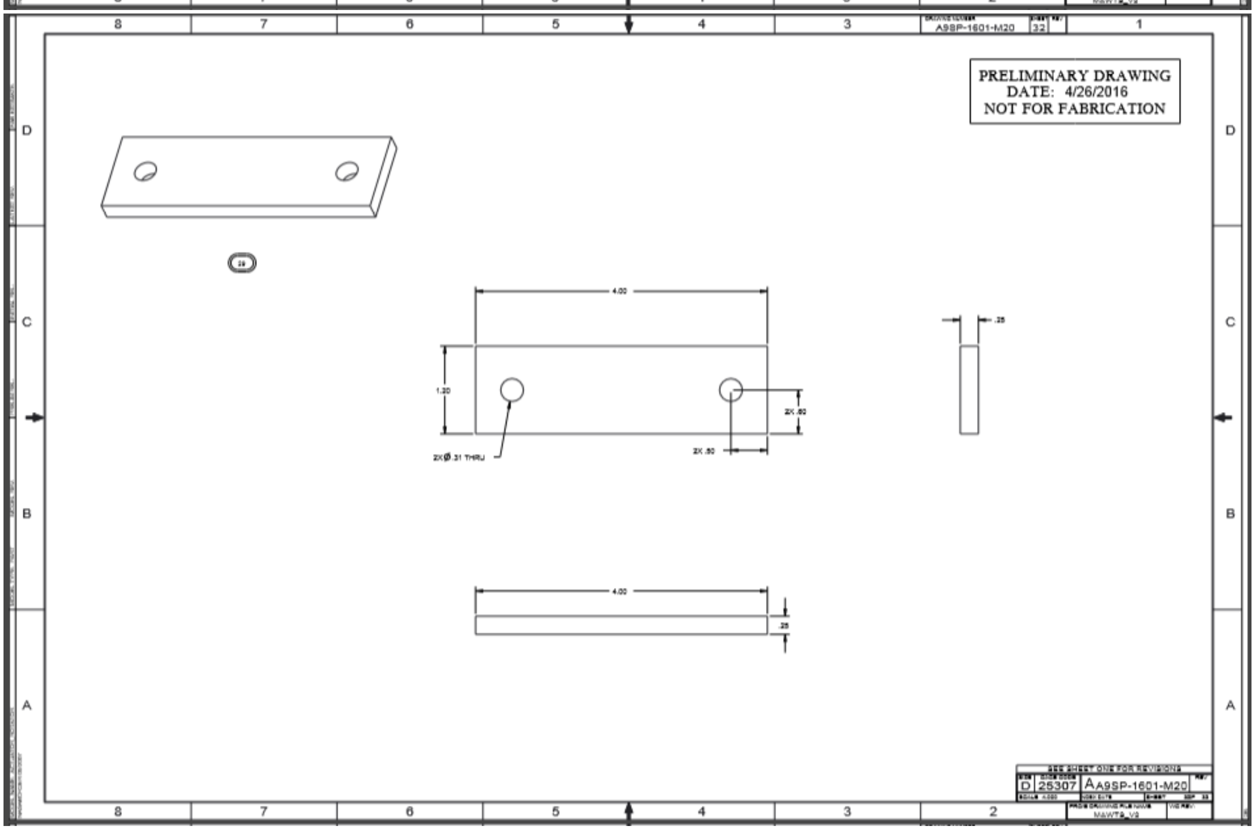
A9SP-1601-M20
32
PRELIMINARY DRAWING
DATE: 4/26/2016
NOT FOR FABRICATION
4.00
1.20
2X Ø.31 THRU
2X .50
2X .60
.25
4.00
.25
D 25307 AA9SP-1601-M20

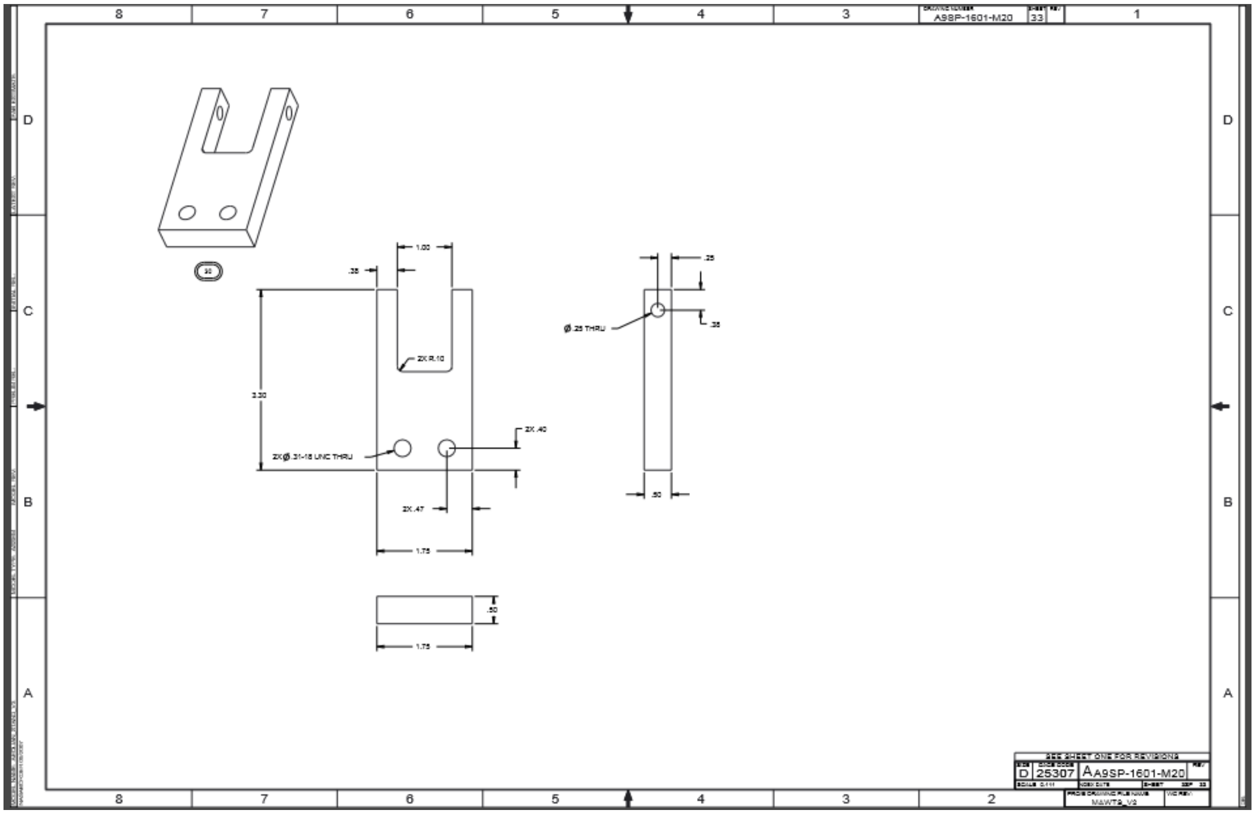
A9SP-1601-M20
33
1.00
.35
.25
Ø.25 THRU
2X R.10
3.30
2X .40
2XØ.31-18 UNC THRU
2X .47
.50
1.75
SEE SHEET ONE FOR REVISIONS
D
25307
A9SP-1601-M20
MAWTS_V2